Journal of the Air Transport Research Society 3 (2024) 100029

Contents lists available at ScienceDirect

Journal of the Air Transport Research Society

journal homepage: www.elsevier.com/locate/jatrs

Modelling the impact of introducing first-generation narrowbody hydrogen aircraft on the passenger air transportation network in Europe

Alexander Rau[a,*], Eike Stumpf[a], Marc Gelhausen[b]

[a] Institute of Aerospace Systems (ILR), RWTH Aachen University, Aachen, Germany
[b] German Aerospace Center (DLR), Cologne, Germany

ARTICLE INFO

Keywords:
Sustainable aviation
Hydrogen aircraft
Air transportation
Network modelling
Optimization

ABSTRACT

The global aviation industry faces a pronounced challenge to mitigate its contribution to anthropogenic climate change, which is caused by burning fossil fuels. One potential pathway is the transition towards using green hydrogen as zero-carbon fuel. Next to technological, infrastructural, and economical challenges, this would introduce a wide range of operational and infrastructural changes to a system centred around safety and reliability. This study employs a holistic approach and examines these changes from a flight network perspective, focusing on passenger transport in Europe. It utilizes network modelling and linear optimization techniques to determine network changes imposed by the introduction of first-generation narrowbody hydrogen aircraft. The findings are threefold: First, the study shows that the air transportation network can be adequately re-created using demand and direct operating cost optimization only, without considering revenue and airline-specific factors. Second, the introduction of hydrogen aircraft will have substantial impact on network structure, incl. flight frequency, capacity, and stopover routes, depending on seat capacity and range of the hydrogen aircraft design. Lastly, it also shows that airports that have a favourable green hydrogen supply will benefit from the introduction of hydrogen aviation.

1. Introduction

Passenger air transportation brings not only people and cultures closer together by transporting more than 4.3 bn individuals in 2019, but also has a sizable effect on the global economy, driving 3.6 % of global GDP in 2019 (ICAO 2019). At the same time, aviation has a substantial contribution to anthropogenic climate change. In 2019 alone, transporting passengers and goods in the air caused a total of 920 megatons of CO_2 emissions (Graver et al. 2020). Additionally, the combined climate impact of non-CO_2 emissions, such as NO_X, cirrus contrails, soot, and water vapor, could be even higher than the impact of CO_2. In relative terms, aviation is only responsible for 2.4 % of global CO_2 emissions, or an estimated 3.5 % of anthropogenic total climate impact (Lee et al. 2021). However, forecasts expect air transportation volumes, measured in Revenue Passenger Kilometres (RPK), to more than double from 2019 to 2050 (Clean Sky 2 Joint Undertaking 2022). At the same time, the industry is seen as one of the most challenging to decarbonize due to the high-power and low-weight requirement profile of aircraft, which so far can only be reliably met by burning fossil hydrocarbon fuels in turbo-engines (Davis et al. 2018; IPCC 2022; ATAG 2021).

Potential technological solutions to the outlined problem can vastly be categorized into two distinct categories: using sustainable aviation fuels (SAF) to power existing turbo-engines or deploying renewably produced, zero-carbon power sources in new powertrain systems. SAFs consist of hydrocarbon fuels that have a reduced lifecycle CO_2 emissions profile, as they are produced by absorbing carbon from the atmosphere. While SAFs can help to reduce aviation's carbon footprint, they are not seen as the optimal long-term solution due to the inability to reach 100 % lifecycle CO_2 and non-CO_2 emissions reduction, low availability, high power or land use requirements, and high cost (Kallbekken & Victor 2022; Ueckerdt et al. 2021; Adler & Martins 2023). Solutions using new powertrain systems can be categorized into battery-electric, hydrogen-powered, or a combination of both. Although full battery-electric systems can eliminate all carbon emissions with maximized well-to-wing efficiency, current and predicted gravimetric battery power density is not expected to exceed meeting short-distance mission requirements, which translate to only a small share of global aviation's emissions. Hydrogen on the other hand has a ~2.8x gravimetric power density of jet fuel and its specific cost per power unit is projected to reach parity with jet fuel by 2050, while having a zero-carbon footprint when produced with renewable energy ("green" hydrogen) (Choi & Lee 2022). It is therefore seen as the least expensive and most sustainable way to fly without carbon in the long term (Timmons & Terwel 2022; Sacchi et al. 2023; Hoelzen et al. 2022), if cur-

* Corresponding author.
E-mail address: alexander.rau@rwth-aachen.de (A. Rau).

https://doi.org/10.1016/j.jatrs.2024.100029
Received 3 May 2024; Received in revised form 10 June 2024; Accepted 13 June 2024

rent challenges with scaling up green hydrogen production can be overcome. Therefore, interest in developing a hydrogen-powered aircraft has gained considerable traction in recent years (Clean Aviation Joint Undertaking, 2021; Airbus 2020; Wood et al., 2023; Rompokos et al. 2020; Stautner et al. 2022; Ling-Chin et al. 2024).

However, replacing jet fuel with green hydrogen will have an enormous impact on the whole aviation system. First, developing such an aircraft still carries a wide array of technological and economical challenges to aircraft design (Adler & Martins 2023). Although existing jet engines could be modified to burn hydrogen, non-CO_2 emissions from the combustion process would still be produced. To eliminate all emissions except for water vapor, a hydrogen-electric powertrain using fuel cells would need to be designed, which however currently still has thermal and specific power constraints. Also, hydrogen would need to be cooled and stored as cryogenic liquid at 20K (-253°C) to maximize volumetric power density. This requires a re-design of the whole fuel system as well as integration of the fuel tanks into the fuselage, introducing an array of new challenges to structural and aerodynamic design of the aircraft. First-generation hydrogen narrowbody aircraft will therefore likely have reduced mission capabilities compared to conventional aircraft, including lower design range, lower seating capacity, lower cruise speed, and higher relative energy requirements. This assumption is reinforced by the announced concepts for hydrogen aircraft designs centred around the smaller aircraft segment (e.g., Airbus 2020).

Second, introducing liquid hydrogen (LH_2) has a considerable impact on the aviation infrastructure (Hoelzen et al. 2022). The entire supply chain, including green hydrogen production, transport, liquefaction, storage, up to the refuelling process at the aircraft, needs to be re-designed. Since green LH_2 production cost depends on renewable energy supply, infrastructure providers need to fundamentally change their fuel supply strategy. Compared to jet fuel, this will likely change the local fuel supply economics. Also, the intensity and timing of airports investing in green hydrogen infrastructure may differ based on strategic considerations and local policy making. Lastly, handling liquid hydrogen may introduce a new layer of safety procedures, for example at aircraft refuelling, potentially affecting turnaround procedures and terminal layouts. In a system centred around safety and reliability, changes in aircraft design as well as adaptations in the air transportation infrastructure will therefore substantially impact how passengers are transported. This study aims to identify this impact and model how the flight network in Europe changes given the introduction of different first-generation narrowbody hydrogen aircraft configurations.

The research approach is structured into six main sections. Following the introduction and literature review in Sections 1 and 2, the fundamental modelling methodology using network theory including all relevant input parameters is explained in Section 3. In Section 4, the optimization model to minimize system cost will be formulated. In Section 5, the network changes imposed by introducing hydrogen aircraft is then analysed, including a comprehensive parameter variation. Finally, Section 6 summarizes findings and provides an outlook to future efforts regarding the subject. All abbreviations are explained in Table 4 in Appendix A.1.

2. Literature review

Although developing a hydrogen-powered aircraft is not a new idea (Brewer 1991; Airbus Deutschland GmbH 2003; Verstraete 2009), examining technological mitigation pathways to reduce aviation's environmental impact using hydrogen has gained considerable traction in recent years. Adler and Martins (2023) and Tiwari et al. (2024) compile an extensive overview of current literature and industrial projects concerning hydrogen in aviation, while Hoelzen et al. (2022) and Degirmenci et al. (2023) outline corresponding infrastructural challenges. Troeltsch et al. (2020) and Huete et al. (2021) develop long-haul widebody hydrogen-powered aircraft concepts to minimize climate impact. Thonemann et al. (2024) focus on hybrid-electric aircraft and alternative fuels to decarbonize the regional segment. Svensson et al. (2024) develop a model for a regional fuel cell electric aircraft and examine its market potential in Scandinavia. Prewitz et al. (2020) determine minimum required gravimetric storage density for a regional fuel-cell electric aircraft to meet a specific design range. Smith and Mastorakos (2024) take an energy system's view to compare LH_2 & fossil fuel powered aircraft in 2050. Oesingmann et al. (2024) calculate liquid hydrogen demand and CO_2 emissions reduction potentials for several aircraft entry-into-service (EIS) scenarios.

While the outlined studies either take a review perspective, limit their scope on regional aviation, or focus on a specific sub-system, none have addressed a holistic assessment of the impact of introducing narrowbody hydrogen aircraft onto the flight network. Even beyond the scope of liquid hydrogen, literature on the impact of new aircraft technology on the flight network is scarce. While some studies examine the interplay between new aircraft design and network layout (e.g., Birolini et al. 2021; Fregnani et al. 2020; Taylor & Weck 2007), others analyse the given network to derive requirements for next-generation aircraft (e.g., Tay et al. 2018; Hwang & Martins 2016). Furthermore, most research focuses on airline-specific networks, while emissions reduction is a system-wide issue.

This study therefore aims to address this gap and show that the air transportation network can be modelled on an overarching, airline-independent level. Following this framework, the study seeks to provide insights on how the flight network structure, in terms of flight frequency, capacity, and stopover routes, changes following the introduction of five different narrowbody hydrogen aircraft configurations. Lastly, the change in significance of specific airports will be investigated. This novel approach aims to contribute to literature and practice by introducing a new methodology to model the air transportation system with the goal of improving the system holistically rather than within sub-system boundaries. It also aims to demonstrate both feasibility and challenges of introducing hydrogen-powered aircraft into the system.

3. Air transportation network

Air transportation is a network industry (Button and Stough 2000; Zanin and Wandelt, 2023). One crucial factor to how air transportation networks emerge is the demand of individuals or goods for transportation from one place to another. The resulting structure of the air transportation network is determined by the "concurrent actions of airline companies, that try, in principle, to maximize their immediate profit" (Guimerà et al. 2005, p. 7794). Airlines operate under several constraints, such as available airside infrastructure including airports, regulatory restrictions, safety protocols, and, most notably, the available aircraft technology. In fact, the dependency between aircraft and network is so strong that "it would be difficult to determine the direction of causality" (Kanafani 1981, p. 306). At the same time, demand is not only a determining factor, but a result of network structure, as passengers are influenced by air fares and connectivity, among other factors. Due to the multi-dimensionality and reciprocity of interdependencies, modelling and understanding the network poses a serious challenge to research and practitioners. A promising approach is applying the logic of complex systems theory to the field (Sallan and Lordan 2020).

3.1. Fundamental network model logic

Complex systems can be represented and analysed using network graphs (Goedeking 2010). Accordingly, a complex network is conceptualized as a weighted graph denoted as $G = (N, E, W)$, where N is a set of N nodes that represent airports, and E is a set of pairs of nodes constituting the links, symbolizing relationships between entities. The quantities of nodes and links are designated as N and E, respectively. Furthermore, the graph is characterized by a set of real numbers W, representing weights associated with each link. Alternatively, the graph

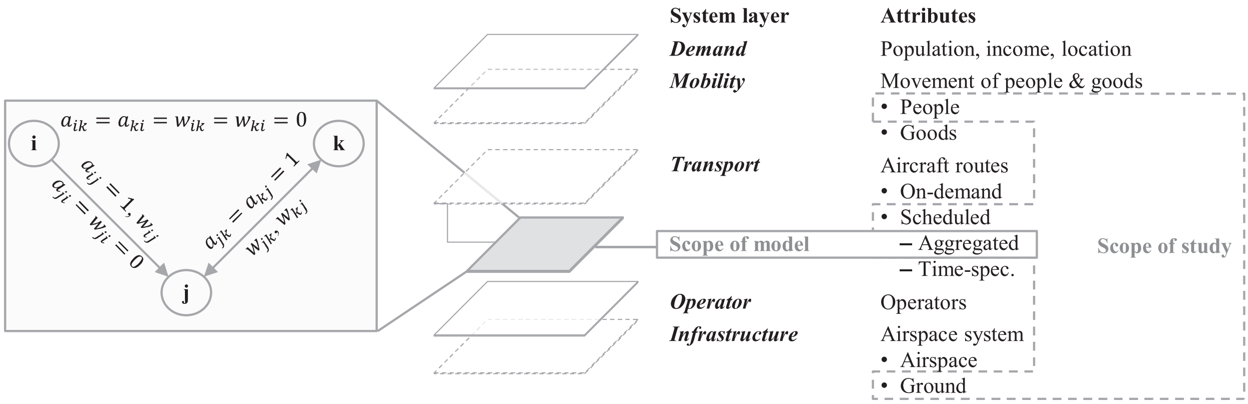

Fig. 1. Level of analysis of the network model, concept based on Bonnefoy, Weibel (2006, p. 4).

can be exhaustively described through its adjacency matrix $W = [w_{ij}]$, a square $N \times N$ matrix with components w_{ij} set equal to the weight of the link between nodes i and j. The non-weighted adjacency matrix is $A = [a_{ij}]$, where $a_{ij} = 1$ if node i and node j are connected, and 0 otherwise (Sallan and Lordan 2020). These networks can then be analysed according to their structure. Several indicators for network centrality are introduced in the literature, of which degree, flow betweenness, eigenvector, and closeness centrality will be used for this study. The meaning and calculation logic of these measures can be found in Table 5 in Appendix A.1. The justification for choosing these specific indicators over several others existing in literature can be found in Cheung et al. (2020).

In air transportation networks, graph nodes represent airports and a link between two nodes is created whenever a direct flight between the two airports associated with the nodes exists. These networks are also called flight networks. Links can be directional, multi-dimensional, and weighted to include relevant information such as passenger and flight numbers, deployed aircraft, or other meaningful information to enhance the network model. Using this scoping approach, the level of detail can be adjusted according to the overarching research goal (see Fig. 1). This study focuses on the movement of people and incorporates scheduled flights due to data availability. Movement of goods is partly incorporated by considering belly cargo, while full cargo operations are excluded due to data availability and the lower relative emissions contribution. This is done on an aggregated level only, neglecting day-time-specific aircraft movements to reduce system complexity. Operator-specific characteristics are omitted to analyse the network from a holistic, systematic viewpoint. The study incorporates ground infrastructure prerequisites to account for changes through the introduction of hydrogen aviation.

Accordingly, node and link data are thoughtfully selected. Specifically, node or airport characteristics are based on open-source data and include IATA-code, metropolitan served and geographic data (latitude, longitude degree).[1] Node specific costs such as fuel and other fees are added according to assumptions from the DOC model (see below in this Section). Link weights include geographic distance between nodes, total number of seats, deployed aircraft type, and total number of flights, which is based on Cirium (2019) flights schedule database. Using a systemwide average load factor assumption, the total number of transported passengers can be estimated.[2] Direct operating costs and CO_2 emissions are calculated based on the aircraft deployed using the fleet/emissions and DOC model (see below in this Section).

[1] Based on https://ourairports.com/data/, last accessed on 26.06.2023.
[2] For 2019, this is assumed at 82.6 %, based on IATA 2020a.

3.2. Available fleet

The deployed aircraft type is a determining factor for various weights, such as number of seats, emissions, direct operating costs, etc., and hence its characteristics need to be modelled thoroughly. The available **fleet size by type** in 2019 is based on Cirium Fleets Analyzer as of 01/2020 (Cirium 2020). The future fleet development is modelled on an aircraft type level using the 2019 fleet as basis, a yearly retirement trajectory until 2050, and a yearly production forecast until 2050. All corresponding assumptions can be viewed in Tables 6 and 7 in Appendix A.2. The retirement trajectory is based on a fixed retirement age assumption, leading to a variable yearly rate per aircraft type based on the number of aircraft that have reached the assumed retirement age. Retirement age is assumed at 25 years, representing the historical average of aircraft age when written off or retired. Age distribution of the existing fleet is taken from Cirium Fleets Analyzer as well. The yearly production forecast per aircraft type is taken from TEAL Aircraft Delivery Forecast until 2026 (TEAL 2023), and afterwards extrapolated using a general annual production growth rate, which is backwards estimated so that the fleet size ratio of 2050 vs. 2019 matches that of the projected number of flights. Lastly, the assumptions for end of production dates of current aircraft and entry-into-service dates for future aircraft are estimated based on literature research (Clean Sky 2 Joint Undertaking 2022). Production rates are transferred to the new-entry aircraft that replaces the existing one. Total number of aircraft in 2050 is estimated to reach 53,177, of which 77 % are narrowbody, 17 % are widebody, and are 6 % regional aircraft. Neo-generation (B737MAX, A320neo, B787, A350) will still represent the largest part of the fleet with 56 % total share, while the adoption rate of next-generation conventional aircraft (“HECA”) is increasing, reaching 36 % of the fleet by 2050. In this forecast, battery-electric regional aircraft are expected to outnumber conventional turboprop aircraft shortly after 2050.

Aircraft **type characteristics** are accumulated from several available sources. Weight and engine characteristics, such as maximum takeoff weight (MTOW), operating empty weight (OEW), number of engines, engine weight, and engine thrust are based on the OpenAP data base developed at TU Delft, which contains 34 of the most common aircraft types and their standard engine configuration, and is based on original manufacturer specifications (Sun et al. 2020). The remaining aircraft type characteristics are complemented based on publicly available data from manufacturers or secondary data sources. Maximum aircraft range is calculated by assessing the maximum route distance of all of the routes that a specific aircraft type was allocated on, according to the flight schedule database from 2019.

The seating capacity per aircraft type represents a crucial part of the network model since it determines required flight frequencies and the number of required aircraft per type. Seating capacity however can dif-

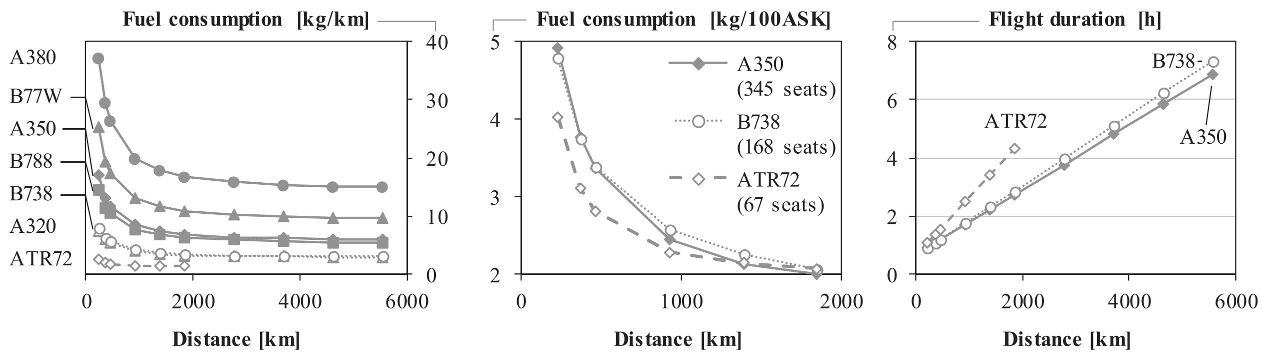

Fig. 2. Specific fuel consumption and flight duration data from EMEP/EEA data base for different aircraft types.[3]

fer substantially even for the same aircraft type, depending on the airline business model. Consequently, average seating capacities are based on a weighted average from the flight schedule database, validated using the fleet database, and manually adjusted for large deviations.

Aircraft **fuel consumption and CO_2 emissions** are calculated as a function of aircraft type and route distance using the EMEP/EEA air pollutant emission inventory guidebook from 2019 (European Environment Agency 2019). This model is based on the Advanced Emission Model (AEM) developed by the European air traffic management organization EUROCONTROL and uses a combination of measurements and estimation models as input to estimate fuel burn and corresponding emissions. The data is widely used for emissions calculation in research (e.g., Yirgu & Kim 2021; Choi & Lee 2022; Ekici et al. 2023) and includes emissions data for the standard or most common engine configuration of 130 aircraft types. For each aircraft type, the data exhibits fuel burn and CO_2 in kg as function of the flight distance. It also shows flight duration per aircraft type depending on the distance (see Fig. 2). The data is split into Landing and Take-Off and Climb/Cruise/Descent flight phases, of which the former is constant for each aircraft type and the latter is a function of the flight distance. For the model, both phases are added up, interpolated with regards to the final distance scale and transformed into three different tables with flight duration on one axis and aircraft type on the other axis: fuel consumption, CO_2 emissions, and flight duration.

One limitation of the emissions data set is that it does not include the latest generation of narrowbody aircraft types such as the A320neo or B737MAX. Since those types represent an evolutionary derivative of existing aircraft types, a relative improvement factor assumption is introduced compared to the existing aircraft types. Based on manufacturer data, fuel and CO_2 emissions efficiency gains over the previous aircraft generation is set at 17 % per seat on average (Airbus 2024; Boeing 2024; University College London). Complementing the data set for future aircraft developments, an assumption on the potential fuel efficiency gains of future aircraft generations has to be made. To account for future aircraft improvements, the same factor is applied as for the A320neo or B737MAX per-seat improvements. This assumes a more fuel-efficient engine, reduced drag, e.g., via active flow control, and reduced vehicle weight, enabled by enhanced materials and structures design. For potential future zero-emission battery-electric aircraft, Mukhopadhaya and Graver (2022) estimate specific fuel efficiency in cruise to be 2-3x higher for battery-electric aircraft, depending on the size of the aircraft. When incorporating take-off, taxi and landing, this study assumes a 1.8x lower fuel consumption of an electric 75-seat aircraft compared to a conventional turboprop aircraft type. Fuel consumption of hydrogen aircraft are discussed in Section 5.1.

3.3. Direct operating cost (DOC)

Total direct operating costs (DOC) are estimated based on the “TU Berlin DOC Method” from Scholz, Thorbeck (2013), which was refined at the ILR of RWTH Aachen to establish a standardized DOC calculation for the Central Reference Aircraft data System (CeRAS) and adjusted for this study’s purpose (Risse et al. 2016). For this, DOC is calculated on a per flight route, deployed aircraft type, and yearly basis (network link), which takes route distance, fuel cost, and aircraft type characteristics (weight, CO_2 emissions, fuel consumption profile, number of seats, etc.) as input. In this conceptualization, DOC comprises fuel cost, navigation, landing and ground handling fees, maintenance costs for airframe and engine, aircraft crew salaries, as well as capital costs for depreciation and insurance:

$$\boldsymbol{DOC}_{flight} = \boldsymbol{DOC}_{fuel} + \boldsymbol{DOC}_{fees} + \boldsymbol{DOC}_{maintenance} + \boldsymbol{DOC}_{crew} + \boldsymbol{DOC}_{capital} \quad (1)$$

The detailed calculation logic and assumptions can be found in Tables 8 and 9 in Appendix A.3. All values, including future projections, are calculated in 2019 Euro levels (real terms).[4] One of the central determining factors of total DOC is specific fuel unit cost, which is furthermore subject to change with the introduction of hydrogen aircraft. The following Section will therefore focus on this part of the DOC model.

3.4. Fuel unit cost

Since fuel cost represents one of the largest operating cost categories for the airline industry, fuel unit costs have to be assessed thoroughly. They are modelled as a function of fuel type (jet fuel, SAF, green liquid hydrogen, renewable electricity), year (2019-2050), and location (airport). Specific fuel prices are estimated using the 2019 levels as basis. Week-wise averaged jet fuel price in 2019 was 1.88 US$/gallon (0.68 €/kg), according to Flightglobal (2022). While **jet fuel** at the refinery can be considered a commodity with volatile price development but limited price variation between regions, the price can differ locally at the airport depending on various factors such as national taxes, airline negotiation and purchasing power, supply competition, distribution technique, etc. (Tabernier et al. 2021, p. 12). However, for the purpose of this study, the jet fuel price at the refinery will be used in the model independent of the airport location. The number of macro- and microeconomic factors influencing commodity prices makes it highly speculative to forecast crude oil and jet fuel prices in the long-term. While the U.S. Energy Information Administration (EIA) expects jet fuel prices to increase by 1.3 % p.a. compared to 2019 (EIA 2020), the Federal Aviation Administration (FAA) expects prices to remain roughly constant until 2042 (FAA 2022). The International Energy Agency (IEA) differentiates scenarios and assumes a slight increase in crude oil prices until

[3] A320: Airbus A320-233; A350: Airbus A350-941; etc.

[4] Exchange rate assumed at 1.0871 €/US$, based on European Central Bank 2023. All assumptions in the TU Berlin DOC model are from 2010 and based on European price levels, hence the 2019 values are adjusted according to the accumulated consumer price index increase from 2010 to 2019 in the EU of approximately 13.1 %, based on The World Bank 2023.

2050 only in the Stated Policies scenario, a flat development in the Announced Pledges scenario and a sharp decrease in the Net-Zero by 2050 scenario (IEA 2021, p. 16). Given the large spread of forecasts, the price for jet fuel will be assumed constant at 2019 levels in real terms, in line with recent studies within the industry (Clean Sky 2 Joint Undertaking 2022; FAA 2022).

An additional factor influencing jet fuel price is the drop-in ratio of **sustainable aviation fuels (SAF)** and the corresponding average SAF price. While the adoption of SAF in 2019 was negligible, the ReFuelEU target ratio is 63 % by 2050, which will be adopted as the SAF drop-in ratio in 2050 in the model (European Commission 2020). While production costs of SAF are expected to decrease, prices for SAF are projected to remain substantially higher than conventional jet fuel. This is based on the assumption of more expensive and limited feedstock for bio-based SAFs, and the high energy requirements for PtL-based SAF. Studies assume factors of 2-8x currently and 1-2x in 2050 compared to jet fuel, depending on the SAF pathway (Graver et al. 2022; ATAG 2021). This does not include subsidies for SAF or cost penalties for carbon emissions. In this study, a factor of 1.5x will be applied to SAF compared to conventional jet fuel in 2050. A sensitivity analysis on SAF and jet fuel prices will be conducted.

Green liquid hydrogen unit prices are adopted from Hoelzen et al. (2023), where green hydrogen cost at the dispenser at 104 European airports was comprehensively assessed based on local renewable energy prerequisites and supply costs. The study minimizes hydrogen supply costs for each airport considering several supply options, including production on site, as well as supply via truck, vessel, or pipeline. Prices range from 1.94 to 2.99 $€_{2019}/kg_{LH2}$, corresponding to a markup of between +3 % and +59 % compared to the 2019 jet fuel price per energy unit. Supplementing these findings, airport availability data (additional to the 104 airports from above) is obtained from Wiener et al. (2023), in which a broad assessment of hydrogen adoption pathways at European airports was conducted. Missing hydrogen costs at airports are estimated with the maximum price within the corresponding country.

Renewable electricity prices for battery-electric aircraft depend on the annual consumption and location (Hospodka 2021). Local availability of renewable energy sources and the national grid price including taxes and levies for green electricity can differ substantially between airports. Combined with consumption-based categorization, the range for non-household consumers in the first half of 2019 spanned from 0.057 $€_{2019}$ in France for Band IG (highest consumption range) to 0.378 $€_{2019}$ in Italy for Band IA (lowest consumption range) (EUROSTAT). Assuming the highest energy consumption range to guarantee a cost advantage for battery-electric aircraft, an average electricity price of 0.06 $€_{2019}$/kWh will be assumed, corresponding to an increase of +6 % compared to the jet fuel price on a per energy basis.

On top of the production price at the dispenser, the final fuel price for airlines might be influenced by positive or negative **taxes**, depending on local policies. These taxes can come in forms of either incentives for buying emissions-reducing fuels, such as green hydrogen or SAF, or penalties for purchasing fossil fuels. While the Inflation Reduction Act (IRA) issued by the United States Government in 2022 used the former to substantially incentivize the production of green hydrogen and bio-fuels (United States Congress 2022), the European Union focuses increasingly on the latter in forms of the Emissions Trading Scheme (EU ETS), which effectively puts a price on carbon emissions above a certain allowance threshold (Efthymiou & Papatheodorou 2019). In the long-term, this study assumes a policy mechanism that makes green hydrogen and SAF competitive with jet fuel to incorporate the political will to become climate neutral by 2050 – irrespective of the final form of the mechanism. A carbon price on top of the jet fuel price will therefore be introduced of 150 $€_{2019}/tCO_2$. This would increase current (2019) jet fuel prices by approximately +70 %. It is not specified if this will be a penalty on jet fuel or an incentive on SAF and green hydrogen.

3.5. Capacity constraints

Independent of the airside hydrogen infrastructure, there are general infrastructural challenges for airports in Europe, mainly centred around capacity constraints (Gelhausen et al. 2021). The airport capacity constraints in terms of flight movements at major European airports have been assessed by DLR (see Gelhausen et al. 2019) and are available for the years 2020 and 2050, including planned runway and terminal extensions. For other airports, real movements at that station in 2019 are applied for 2019 with a 20 % markup to allow for flexibility in the optimization. For 2050, figures are extrapolated consistent with the overall demand growth. Due to remaining uncertainty with regards to the final extent of capacity constraints, two scenarios are considered, including a standard parameter case, and one with increased airport capacities, subject to a sensitivity analysis.

3.6. Modal shift

Modal shift to ground transportation plays an important role in decarbonization pathways of the transportation sector in Europe (European Union 3/28/2011; Brons et al. 2023). Particularly for short-distance travel, ground transportation substitutions potentially influence the future air transportation network. In Europe, ground transportation is generally estimated to be a valid substitute for routes with land connection and distances below 400-500 km (Baumeister 2019; Prussi & Lonza 2018). Due to aircraft-specificity of the DOC model and high dependence on passenger preference, the ground transportation DOC profile is constructed in relation to novel aircraft type alternatives and must be considered as relative cost curve rather than actual ground transportation DOC (see also Sun et al. 2018). It uses a linear progression with two main anchor points: Below 150 km, where ground transportation is perceived as more convenient than flying and the assumed per-seat cost is lower than for all in-service aircraft. And above 300 km, in which travel times become more inconvenient than using the reference hydrogen aircraft option.[5]

3.7. Network model result for 2019

Fig. 3 shows the resulting global network based on the previously outlined modelling methodology and input parameters. Although the analysis of this study is focused on the European sub-system (see Section 4), validation of the as-is network incorporates the global network to demonstrate the global applicability of the approach. The network graph has 3,992 nodes (airports), 155,320 directed multi-links (Origin-Destination-Aircraft combinations), 61,604 directed links (Origin-Destination combinations), and 31,515 undirected links (Origin-Destination pairs). The average degree per node is 15.8, indicating that the average airport has direct connections to roughly 16 other airports. This is however not equally distributed, as the degree distribution follows the common understanding of a “heavy-tailed” network. This means that a small number of nodes have a very high degree (so-called hubs), while most nodes have very few links. In terms of overall travel volume, the total ASK modelled in the network sums up to 10.38 tn seat-kilometres, which is within a 0.5 % error margin compared to IATA’s estimate (10.43 tn ASK). Number of flights (38.3 m) and number of seats provided (5.7 bn) are also in line with the industry association’s estimate (IATA 2020b). Assuming a system-wide load factor of 82.6 % (industry average in 2019 according to IATA), the overall passenger volume is 4.7 bn, and global RPK is 8.58 tn (vs. 4.5 bn and 8.68 tn). In terms of DOC, the global airline industry had a total operating expense of 795 bn US$ / 731 bn $€_{2019}$ including passenger and cargo operations in 2019 (IATA 2022). Excluding ticketing, sales and promotion

[5] To guarantee comparability between scenarios, $H2^A$ will be taken as reference hydrogen aircraft for all scenarios.

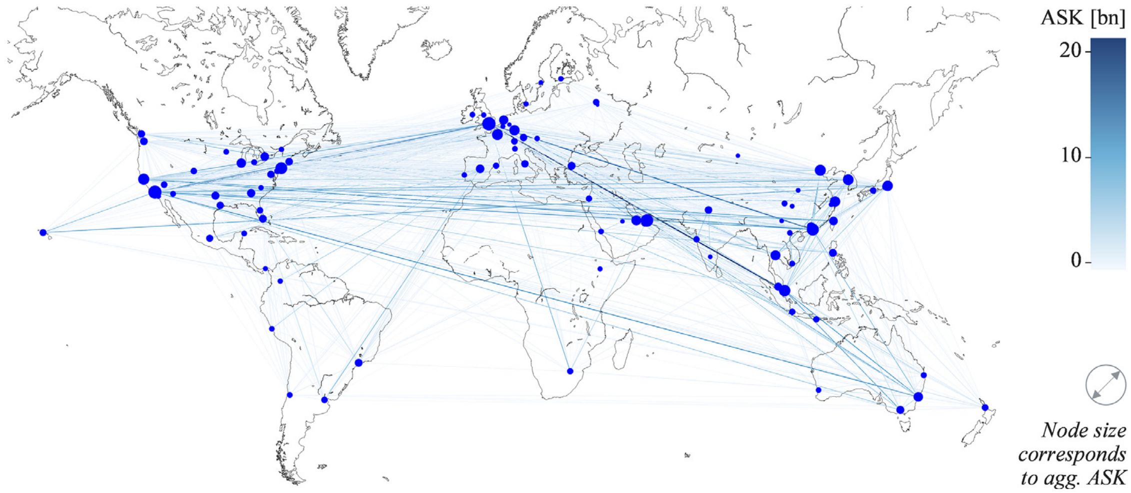

Fig. 3. Network model with top one hundred airports by aggregated ASKs.

cost, general and administrative cost, and other expenses as well as dedicated freighter cargo operations, the total operating expense of the air transportation industry can be estimated at 553 bn $€_{2019}$ (IATA 2020b). Applying the DOC model onto the network model for 2019 based on Cirium scheduled flights data, a total direct operating cost of 561 bn $€_{2019}$ is calculated, which is located within a 1.5 % error margin compared to the estimated industry actuals. Relative shares of the cost blocks within direct operating costs are also within reasonable error margins.

4. Network optimization model

The goal of the optimization model is to simulate the reaction of the air transportation network to changes in fleet composition, given a specific demand for transportation. Since the goal of network operators is to minimize operating costs if revenues are constant, the network should follow a logic in which the lowest direct operating costs are achieved, given their respective constraints. Therefore, a demand-to-aircraft-to-flight allocation optimization model will be deployed, in which direct operating costs (DOC) are minimized. The optimization will have three different layers: demand, assignment options, and flight network (or "supply"). Demand between two city pairs is assumed constant and needs to be met by the resulting air transportation network. The demand can be met by either a direct connection or a stopover connection. Multi-stopover connections are not in scope of this study to minimize model complexity. For each city pair of the network in scope, there are several demand-to-aircraft-to-flight allocation options (second layer). This means that there are several ways to meet each demand item from city A to city B, varying in origin and destination airport within the metropolitan areas, aircraft used, and stopover airport (*None* for a direct flight). These options represent an intermediate level between the demand and the flight network. Allocating one passenger demand unit to an aircraft allocation option increases the frequency and number of aircraft required on the flights this option makes use of. More precisely, the model has two connecting layers between the three layers: First, passenger demand items on an origin-destination pair basis are assigned to one of the potential options for each demand item. Second, each option "makes use" of the flight(s) and aircraft associated with it, i.e., either the direct flight or both leg flights of the stopover route (see Fig. 4).

The scope of the model will be focused on Europe due to most promising policy outlook when it comes to the promotion of hydrogen in aviation as well as demand data availability. Although the potential of hydrogen as fuel for aviation is being acknowledged and studied around the world, regulatory frameworks supporting rapid adoption of those fuels are expected to especially prevalent in Europe, in line with the European Commission's ambition to achieve carbon net zero by 2050 (Sacchi et al. 2023). Methodologically, reducing the scope to a relatively mature sub-system of the air transportation system furthermore carries the advantage of reducing problem size and uncertainty, while increasing the ability to interpret the result in a meaningful way. Findings are nevertheless conditionally transferable to other regions as well. The available fleet has to be reduced accordingly. The ratio of utilized aircraft for flights with departure or arrival at European airports compared to the global number of stored or in-service aircraft in 2019 was 20 % for narrowbody aircraft and 36 % for widebody aircraft. Since the share varies per aircraft type, a markup is added for the final maximum aircraft number, leading to 28 % of global aircraft type availability for narrowbody aircraft, and 40 % for widebody aircraft. This leaves an appropriate corridor (+12 % considering a fleet of the most relevant aircraft types with >100 aircraft in service in Europe) for the optimization to choose the most economic aircraft.

One major concern is the handling of system boundaries, as aviation is a highly interconnected and globalized system, in which changes outside defined system boundaries have an effect on characteristics inside the boundaries. A flight-bundling approach is suggested, in which all links going beyond system boundaries are bundled based on geographical communalities. These geographical communalities are grouped using a refined definition of the IATA classification for world regions, splitting Latin America and Africa into North and South as well as North America in West and East. Asia Pacific is split into Central, East, Southeast, and Oceania. The resulting distribution can be found in Fig. 14 in Appendix A.4.

Current and future **origin-destination demand** will be based on own computations derived from MIDT data for OD-demand in Europe from 2019 (SABRE 2019). This data set is based on real flight booking data on an origin-destination basis, independent of the final transportation route, and has been widely used for scientific analyses (e.g., Maertens et al. 2020; Gelhausen et al. 2018). The data set is manipulated to exclusively cover air transportation bookings, omitting demand that is met by modal alternatives, such as ground transportation. For the future network, the 2019 data is extrapolated uniformly using a compound annual growth rate of 2 %. This is based on an average projection between different development scenarios of air traffic growth in Europe incorporating the effects of the COVID pandemic (Clean Sky 2 Joint Undertaking 2022). The approach is justified given uncertainties in relative demand development and the forecast's role as baseline to compare hydrogen scenarios against, not as main subject of examination. To simplify the modelling approach, demand between origin-destination pairs is aggregated to simulate symmetric return trips.

Air transportation **assignment options** are pre-constructed as a solution space for meeting given demand. There needs to be at least one

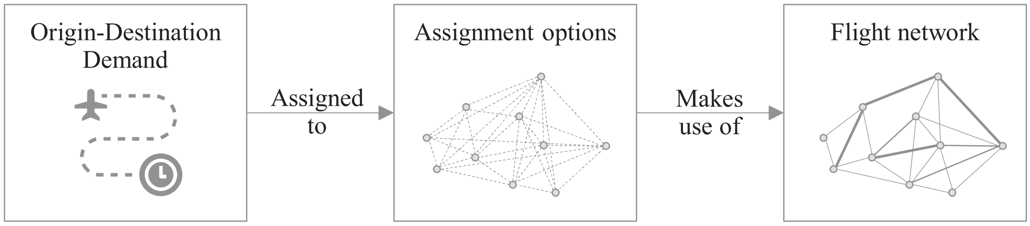

Fig. 4. Network layers within the optimization model.

option to meet each demand item. Options can entail either a direct flight or a stopover connection via a selected set of stopover hubs. The procedure to define the set of options is as follows: The OD-demand data is used to assign a direct connection from and to all airports within the demand metropolitan origin and destination to each demand item. Then low-frequency options are eliminated to reduce the solution space, i.e., only options with demand above one hundred passengers per week on routes above 500 km remain. The underlying rationale is that airlines are not able to operate low-frequency routes profitably, except they are used as short-distance stopover leg. Options that exist in the 2019 real network are excluded from this step. The next step involves creating one-stop stopover routes for each demand item. In general, all combinations of two existing direct options can be used to construct a stopover route. To limit the solution space, the following criteria are enforced: The maximum total distance of both legs must be below a factor of three times of the direct distance for intra-European routes, and below two times for extra-European routes. Furthermore, only eligible stopover airports can be used. Eligible stopover hubs are subdivided into four categories: airline hubs, intra-stopover hubs, extra-stopover hubs, and hydrogen hubs. The complete list and explanation of the different hub types can be found in Table 10 in Appendix A.5. As a last constraint to limit the available stopover options, only options are kept which are ranked in the top twenty options either in terms of lowest total distance of both legs, or highest sum of demand from both legs that are used. Adding stopover routes results in a set of 1.6 m options. The last step involves bundling extra-European trips and aggregating options to simulate symmetric return trips. Finally, the total options set amounts to roughly 450,000.

With in the **flight network** layer, an aircraft type is assigned to each flight link, for which the maximum range cannot exceed geographic distance between the nodes. The number of passengers and the aircraft type deployed then determines the remaining variables, including number of flights, direct operating costs, etc.

4.1. Model formulation

The objective is to minimize total system direct operating costs (2):

$$\min \sum_{a\in A}\sum_{f\in F} \boldsymbol{DOC_{af}} \cdot \boldsymbol{n_{af}} \tag{2}$$

A is the set of available aircraft types, and F is the set of potential flight routes between origin and destination. af represents an aircraft-to-flight allocation option. $n_{af} \in \mathbb{R}_{\geq 0}$ is the floating-point variable for the number of flights per year aircraft a is allocated to perform on flight route f. DOC_{af} represents the total direct operating cost that occurs for conducting one flight on route f when deploying the aircraft of type a. The first constraint (3) enforces that demand d_{od} (number of passengers demanding to be transported between origin-destination pair od) is met:

$$\sum_{r\in R_{od}} \boldsymbol{p_r} = \boldsymbol{d_{od}} \ \forall \boldsymbol{od} \in \boldsymbol{OD} \tag{3}$$

OD represents the set of all origin-destination pairs between which demand for air transportation exists. R_{od} represents the set of all route options between origin-destination pair od. These can be direct flights or stopover routes. Consequently, p_r is the number of passengers assigned to route r. The second constraint (4) enforces that there are enough seats allocated to flights between origin-destination-pairs:

$$\boldsymbol{LF_{max}} \geq \frac{\sum_{r\in R_f} \boldsymbol{p_r}}{\sum_{a\in A} \boldsymbol{n_{Seats,\ a}} \cdot \boldsymbol{n_{af}}} \ \forall \boldsymbol{f} \in \boldsymbol{F} \tag{4}$$

Note that now, R_f represents the set of route options that make use of flight route f. The sum of passengers p_r hence in this case is represented by passengers deployed on the direct route between origin and destination of flight route f, as well as passengers of a different origin-destination pair that use flight route f as first or second leg of a stopover route (see Fig. 5).

LF_{max} is the maximum load factor, subject to model parameter settings, and expresses the ability of airlines to fill seats on existing routes. Increasing the load factor reduces DOC and hence is an inherent goal of the optimization algorithm. Setting maximum load factor therefore incorporates airlines not being able to fully fill their seats due to operational considerations. LF_{max} will be set to 0.83, as in the 2019 network model, which the optimization model will be compared against. The next constraint (5) enforces that the available number of aircraft of type a, $n_{max,a}$, is not exceeded, with FC_{af} representing the number of flight cycles per year that a would accomplish on flight route f.

$$\sum_{f\in F} \frac{\boldsymbol{n_{af}}}{\boldsymbol{FC_{af}}} \leq \boldsymbol{n_{max,a}} \ \forall \boldsymbol{a} \in \boldsymbol{A} \tag{5}$$

Airport capacity limits are enforced by the following constraint (6):

$$\sum_{a\in A}\sum_{f\in F_s} \boldsymbol{n_{af}} \leq \boldsymbol{cap_{max,s}} \ \forall \boldsymbol{s} \in \boldsymbol{S} \tag{6}$$

S is the set of all airports within the network, F_s is the set of flights to and from airport s, and $cap_{max,s}$ represents the maximum annual aircraft start and landing slot limit for airport s.

A shortcoming of the modelling methodology not incorporating revenue and airline-specific factors is that the model inherently prefers direct options as the most economical way to meet demand. In theory, there are however two main reasons for passengers to choose a stopover or indirect route. Either there is no direct option offered at the desired time of transport, e.g., because of lower flight frequencies. Alternatively, the stopover route fare is lower than the direct route fare (Hess 2016). The nature of the model is not designed to depict either of these externalities. As a result, a constraint (7) enforcing more stopover routes is established:

$$\sum_{r_{so}\in R_{so,od}} \boldsymbol{p_{r_{so}}} \geq \boldsymbol{f_{so,min}}\left(\boldsymbol{d_{od}}\right) \cdot \boldsymbol{d_{od}} \ \forall \boldsymbol{od} \in \boldsymbol{OD_{SO}} \tag{7}$$

OD_{SO} represents the set of all origin-destination pairs between which a stopover option exists. This explicitly excludes routes which involve airline hubs (as defined before), as a forced stopover is not sensible for already highly frequented routes. $R_{so,od}$ represents the set of all stopover options between origin-destination pair od. Consequently, $p_{r_{so}}$ is the number of passengers assigned to stopover route r_{so}. $f_{so,min}(d_{od})$ is the minimum passenger stopover share on the route and is reciprocally dependent on the total route demand (8):

$$\boldsymbol{f_{so,min}}\left(\boldsymbol{d_{od}}\right) = \boldsymbol{f_{so,0}} \cdot \left(1 - \frac{\boldsymbol{d_{od}}}{\boldsymbol{d_{max}}}\right) \tag{8}$$

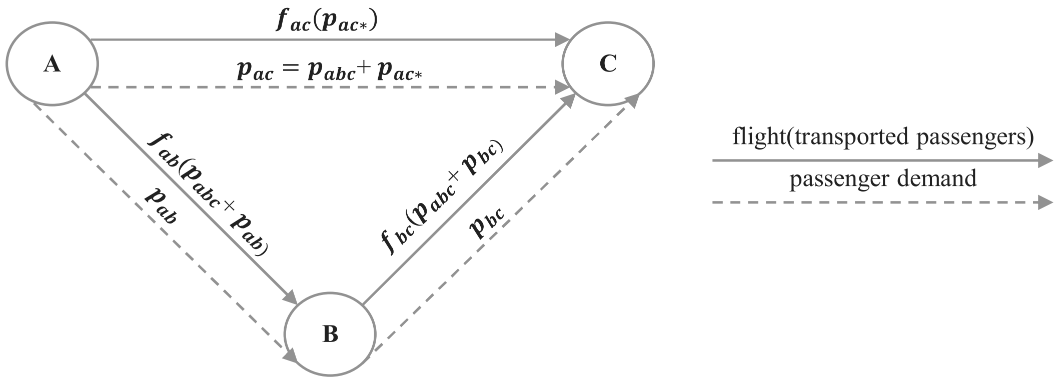

Fig. 5. Model logic for demand and supply with direct and stopover routes.

$f_{so,0}$ is the base value of the minimum stopover share, and d_{max} is the maximum demand item of the system. This way, the highest demand item has a minimum stopover share of zero, because the route will have the highest frequency given constant aircraft size. The stopover share increases for lower demand because the probability of an inconvenient schedule increases.

A second unrealistic model characteristic is a radical search for the most economical option. If there are multiple options with comparable economics, the solver always elects the route option with the lowest DOC and maximizes allocation to this route until it reaches a constraining parameter. In the real world, the selection of stopover routes is more fragmented due to airline competition. Also, the choice of the stopover route is less determined by total distance, but more by schedule. Since both factors are not part of the modelling method, two constraints (9 and 10) enforcing the fragmentation of stopover routes need to be incorporated in the model formulation:

$$\sum_{r_{so} \in R_{so,od}} x_{r_{so}} \geq n_{so_{min},\, od} = f_{so,1} \cdot N(r_{so}) \ \forall\, od \in OD_{SO} \quad (9)$$

$$\left(p_{r_{so}} \geq f_{so,2} \cdot \frac{x_{r_{so}}}{n_{so_{min},\, od}} \cdot d_{od,so} \ \forall\, r_{so} \in R_{so,od} \right) \forall\, od \in OD_{SO} \quad (10)$$

$x_{r_{so}}$ is a new Boolean variable to indicate whether there is a positive number of passengers allocated to stopover route r_{so}. The minimum number of serviced stopover routes $n_{so_{min},\, od} \in \mathbb{Z}$ is a function of the number of available stopover routes $N(r_{so})$ for origin-destination pair od. The factor $f_{so,1} \in [0,\ 1)$ is backwards-determined to yield the highest model fit, ceteris paribus, at two-thirds. This would mean that two out of three available routes need to be serviced. On each of the serviced routes, the number of allocated passengers needs to achieve a minimum threshold, to ensure a levelized distribution between the options. If $f_{so,2} \in [0,\ 1]$ is close to one, the distribution is almost equal. A lower figure would favor the most economic (lowest total distance if all other factors remain constant) route. Varying this parameter shows a higher fit for higher $f_{so,2}$, so that it is set at 0.99 initially (to avoid numerical issues). Note that $d_{od,so}$ represents the minimum demand share that is assigned to stopover routes from constraint (7), i.e., $d_{od,so} = f_{so,min}(d_{od}) \cdot d_{od}$ for routes with both direct and stopover routes. $d_{od,so}$ equals d_{od} for routes that do not have a direct option. Lastly, it has shown beneficial to define the number of available stopover routes $N(r_{so})$ as number of routes with different stopover stations. This way, routes with the same origin and destination, but different departing or arriving airports only count as one contributing route, to avoid a bias for stopover routes with several different airport options.

4.2. Results for the 2019 network validation

The model is solved as a Mixed Integer Linear Programming (MILP) problem using Gurobi Optimizer (version 11.0.1) for the 2019 OD-demand and fleet. The year 2019 is chosen as the last full year without the impact of the COVID-19 pandemic on the air transportation system (Bao et al. 2021). The result is the DOC-optimized passenger-to-aircraft-to-flight network configuration given defined constraints. Compared with the actual, non-optimized network from Section 3.7, the results show a good overall fit, as depicted in Table 1, Figs. 6 and 7. The model explains >91 % of the variation in passengers per route, and >98 % in passengers per airport. Mean absolute error (MAE) per route is approximately 40,000 passengers. The number of flights per route also show a lower, but acceptable model fit at 87 %.

To compare both network topologies, only intra-European connections are considered. Also, a link is only considered if it exceeds a threshold of 26 flights per year (one-way, indicating at least a bi-weekly schedule), to make differences between the networks clearer.[6] Similar to the passenger and flight volumes, the resulting centrality measures demonstrate a high R^2 (see Fig. 7), indicating high similarities in network structure between model and actuals. Average degree increases by +1.2 %, from appr. 23.3 to 23.5, suggesting a slightly higher average connectivity. Notably, the average degree for the top-50 metropolitan stations increases by +6.8 % from 125.3 to 133.8, indicating an overweight for already highly connected airports. Average flow betweenness centrality decreases by -8.2 %, but this is mitigated for the top-50 nodes (-2.9 %), in line with the degree distribution. This indicates a lower likelihood for an average node to be located on the shortest path between unconnected nodes and reinforces the hypothesis of overweight connectivity for already highly connected nodes in the modelled network vs. the representation of the actual network.

The model is able to explain 85.8 % of the variation in closeness centrality, an indicator representing the accessibility of an airport in a network, depending on its mean shortest distance to other nodes. Closeness centrality increases by +0.9 % on average, and +2 % for the top-50 nodes. This means, the model tends to overestimate closeness, especially for already highly connected nodes, confirming findings from prior indicators. The model explains 96 % of the variation in eigenvector centrality, a measure of importance of a node in the network depending on the passenger flow. Average eigenvector centrality increases by +1.2 %. It can be observed that the eigenvector centrality of multi-airport metropolitan areas, such as Paris PAR, Milan MIL, or Moscow MOW, is overestimated, while it is underestimated for single-airport metropolitans, such as Amsterdam AMS, or Frankfurt FRA. Not incorporating airline presence as well as levelized stopover flows might be further contributing factors to deviations in eigenvector centrality, which all need to be considered when evaluating future projections of the network.

[6] The resulting 640 nodes and 7,537 links account for >99% in DOC, number of flights, ASK/RPK and passenger volumes compared to total intra-European values.

Table 1
Model results for the 2019 network.

	Total				Europe			
	Absolute	Relative	R^2	MAE	Absolute	Relative	R^2	MAE
Passengers [bn]	1.36	100%	91%	4.09E-05	1.01	100%	93%	2.76E-05
No. Flights [m]	9.70	99%	87%	3.53E-07	7.93	98%	87%	2.83E-07
DOC [$€_{2019}$ bn]	181.3	98%	-	-	86.1	103%	-	-
Aircraft [#]	7,605	101%	-	-	4,834	98%	-	-

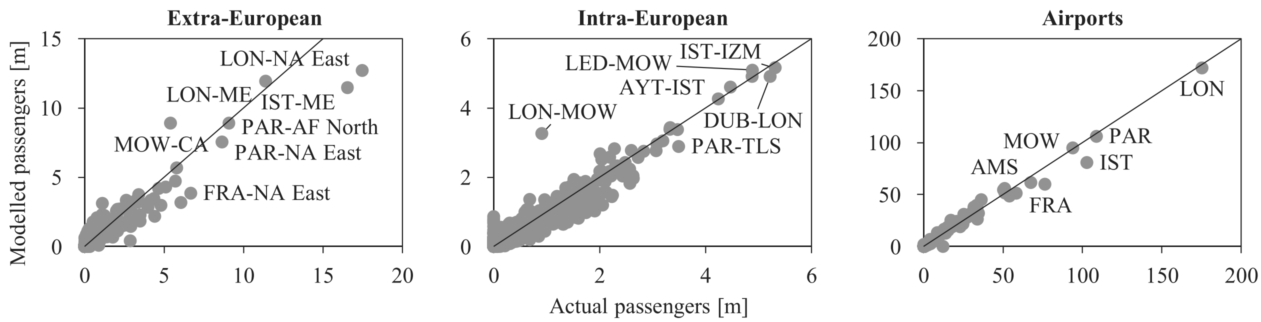

Fig. 6. Comparison of passengers per route & airports[7].

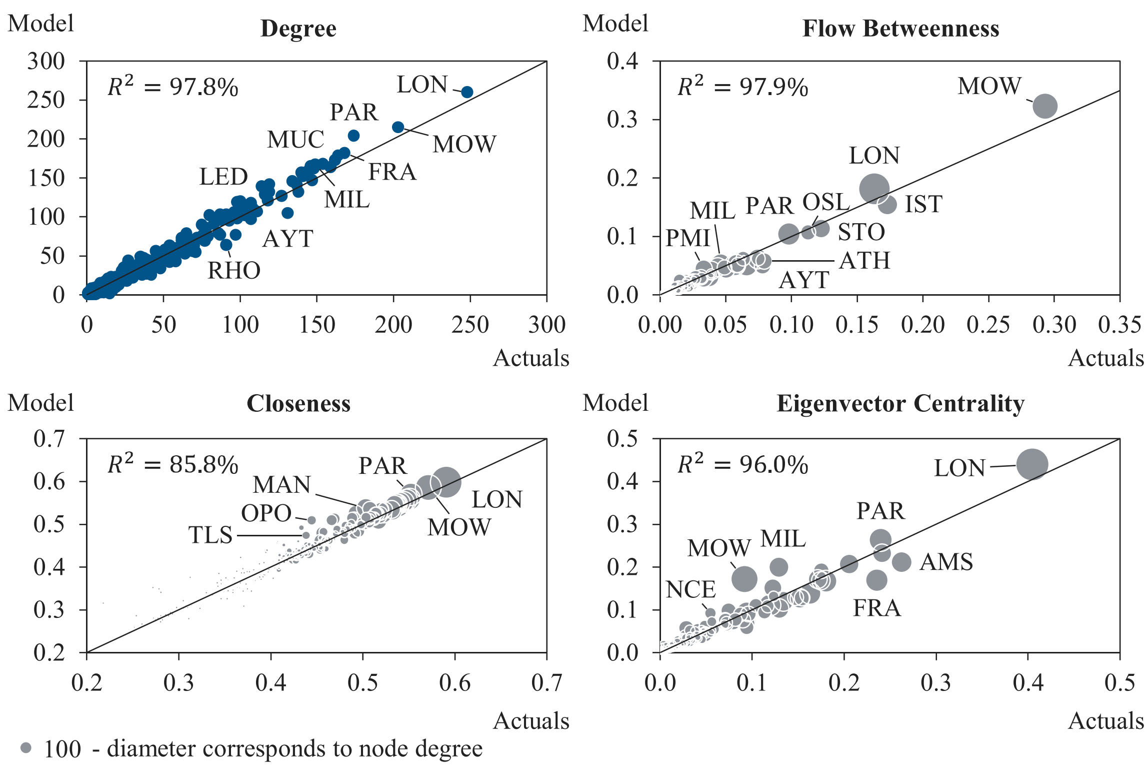

Fig. 7. Comparison of various network centrality indicators, model vs. actuals.

4.3. Forecast to 2050

At first, the forecast will be constructed using standard parameter settings and with modal shift. This also includes the introduction of a zero carbon emissions regional aircraft with 75 seats and 1,000 km range. This scenario assumes a full battery-electric powertrain for this aircraft with maximized energy efficiency to calculate DOC for an extreme case. It is however realistic to assume that this is replaced or complemented by hybrid-electric or hydrogen fuel-cell powertrains that have lower, but still superior energy efficiency compared to conventional powertrains. These aircraft types are also believed to pave the way for narrowbody hydrogen aircraft in terms of technological and infrastructural development. The initial results show that passenger volume increase by +79 % compared to 2019, reaching 2.42 bn passenger-legs (see Table 2). This is lower than the cumulative demand growth (+86 %) as a share of the network is shifted towards ground transportation. Direct operating costs grow slightly above the passenger growth rate since increasing fuel prices counterbalance fleet efficiency savings. At the same time, number of aircraft and number of flights increase

[7] CA = Central Asia, ME = Middle East, NA = North America, AF = Africa.

Table 2
Results of the 2050 forecast in the standard scenario.

	Total			Europe		
	2050	2019	Change	2050	2019	Change
ASK [tr]	7.08	3.85	+84 %	2.64	1.44	+84 %
Passengers [bn]	2.42	1.36	+79 %	1.77	1.01	+76 %
No. Flights [m]	15.75	9.70	+62 %	12.15	7.93	+53 %
DOC [$€_{2019}$ bn]	337.64	181.33	+86 %	162.85	86.09	+89 %
Aircraft [#]	13,620	7,605	+79 %	7,724	4,834	+60 %
CO_2 Emissions [Mt]	328.45	272.13	+21 %	141.19	106.81	+33 %

by +79 % and +62 %, respectively. This is a result of an upsizing of the average aircraft capacity in the fleet forecast, airport capacity constraints, and modal shift. Within Europe, growth in number of aircraft and flights is even more restricted, growing only by +60 % and +53 %, respectively. This also carries an increased growth in direct operating costs within Europe compared to the system level. Noteworthy, airport capacity constraints outside of Europe are not included in the model. CO_2 emissions growth is only a fraction of passenger growth (+21 % on system level), due to a substantially more fuel-efficient fleet, modal shift, and introduction of zero-emission regional aircraft.[8] Within Europe, this dynamic is less pronounced (+33 %), with one explanation being airport capacity constraints.

Fleet upsizing can be observed by the average number of seats increasing to 197 per aircraft (+3 compared to 2019). For narrowbody aircraft, the number increases from 160 to 180, and for widebodies from 296 to 334. In this scenario, the dominant aircraft type by 2050 is the narrowbody neo generation with 52 % of the fleet in Europe. The fleet share of widebodies decreases further, from 25 % to 14 %. The most used narrowbody aircraft type is the A321neo (2,574 aircraft), and the most used widebody aircraft is the 320 seat HECA (1,086 aircraft). The airport with most movements is projected to be Amsterdam AMS (718,113), followed by Istanbul IST (716,688), and Paris CDG (619,713). Barcelona BCN is the largest of nine airports that reach the flight movement capacity limit in the projected scenario. In fact, five metropolitan aera stations reach their capacity limit (BCN, DUB, GVA, TBS, VIE). In these stations, growing demand can only be met by increasing aircraft size.

In an alternative scenario without battery-electric aircraft and ground transportation substitution, the total number of passenger-legs is increasing due to no modal shift. This is especially observable on short routes in dense areas (Central Europe). Especially the Frankfurt FRA airport would have a much higher growth in flight movements (+86,000 flights in total) with the same number of passengers passing through the node. The overall impact is an increase of +2.7 % in number of flights, -1.1 % decrease in aircraft required, and an increase of +2.6 % in CO_2 emissions. This scenario will however not be covered further.

5. Hydrogen aircraft introduction

5.1. Hydrogen aircraft configurations

Table 3 summarizes the different narrowbody hydrogen aircraft introduction scenarios. The introduction of narrowbody hydrogen aircraft is expected to follow the introduction of smaller hydrogen-powered aircraft types for regional applications, which are already part of the standard scenario (refer to Section 4.3). The study focuses on narrowbody aircraft as the carbon emissions reduction potential for regional aircraft types is very limited. The different aircraft configuration scenarios below are based on a comprehensive study on minimum aircraft requirements for a narrowbody hydrogen aircraft from a network perspective with the overall objective of reducing carbon emissions.[9] The scenarios include two fuel-cell electric hydrogen aircraft options and three hydrogen combustion options with EIS in 2035. Range, number of seats, weight, thrust, and specific energy usage E_{req} were determined based on existing literature and proprietary assumptions. In general, performance parameters are inherited from the parent conventional narrowbody aircraft type and scaled with respect to the comparative seating capacity. Detailed explanation for specific assumptions can be found in Appendix A.6.

5.2. Introduction of hydrogen aircraft in the standard scenario

The introduction of hydrogen aircraft into the air transportation network is simulated for each of the pre-defined hydrogen designs. The counterfactual against which the network will be compared is a network with electric aircraft, and ground transportation substitution. Two important alterations have been added to the network optimization. First, new stopover routes are introduced for all airports that do have a hydrogen supply. This enables new airports to emerge as stopover hubs if route economics are favourable. Second, the maximum size of the conventional narrowbody aircraft fleet is reduced to 22 % (-8 p.p.) of the global fleet to consider both reduced production capacities for conventional aircraft as well as accelerated retirement for older, inefficient aircraft of current and neo generation in case a hydrogen aircraft enters the market.

5.3. High-level results

Fig. 8 illustrates the outcome of various network optimizations, depending on the hydrogen aircraft type. Overall, the number of transported passengers via air increases slightly for every configuration reflecting a partial replacement of ground transportation infrastructure. This is attributable to the chosen representation of ground transportation costs, which is assumed higher for distances above 300 km. The underlying rationale is that hydrogen aircraft represent a zero-emission and travel time reducing alternative to ground transportation for larger distances. Moreover, there is a considerable rise in both the number of flights and aircraft required across all configurations. This is a consequence of the lower size of the deployed hydrogen aircraft compared to conventional aircraft. Accordingly, it can be observed that the higher the seat capacity, the lower the increase in number of flights and aircraft becomes. Although LH_2 price is expected to be lower than the jet fuel/SAF mix price in the chosen scenario, changes in direct operating costs (DOC) are negligible. This outcome arises from the lower energy efficiency of combustion-based hydrogen aircraft on a per seat basis, along with other increased operating costs, such as capital expenses. CO_2 emissions are reduced by -15 to -24 % on a system-wide level, and by up to more than -50 % for the intra-European network. $H2^A$ demonstrates the highest CO_2 emissions reduction due to higher seating capacities and better per-seat economics compared to $H1^+$ and $H2^B$. The number of required LH_2 aircraft ranges from 4,430 (H0) to 5,073

[8] In this study, CO_2 emissions are gross emissions, without incorporating the net CO_2 footprint of fuel production.

[9] This analysis will be published separately.

Table 3
Narrowbody hydrogen aircraft scenarios and performance data.

Aircraft type	EIS	Propulsion type	Seats	Range [km]	Parent type[1]	OEW [t]	$MTOW$ [t]	DOC_{cap} [€/ASK]	E_{req} [kW/ASK]
H0	2035	Fuel-cell electric	130	1,500	NB120	35.3	50.5	+12 %	-5 %
H1	2035	Fuel-cell electric	140	2,000	NB150	43.1	61.7	+12 %	-5 %
$H1^+$	2035	Combustion	140	3,000	NB170	45.7	65.3	+12 %	+12 %
$H2^A$	2035	Combustion	150	3,250	NB170	48.9	69.9	+12 %	+12 %
$H2^B$	2035	Combustion	160	2,500	NB170	55.1	79.1	+12 %	+12 %

[1] Parent type corresponds to the technological specifications the respective hydrogen aircraft type inherits. All parent aircraft types assumed to be HECA (Hyper Efficient Conventional Aircraft) generation; NB = Narrowbody; Number corresponds to the number of seats, see Appendix A.6.

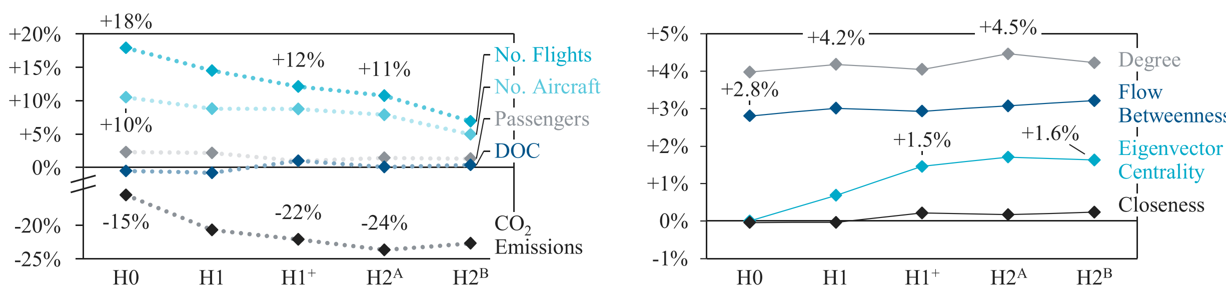

Fig. 8. Relative change of network characteristics for different hydrogen aircraft introductions.

($H1^+$), implying a substantial production requirement within 15 years after EIS. In terms of network disruption, the total accumulated absolute change in passengers per route is considerable. It varies between 390-500 m passenger-legs compared to an overall volume of 2.5 bn. $H1^+$ exhibits the lowest level of disruption, potentially attributable to the greater similarity in configuration to existing aircraft like the A220. The highest disruption can be measured with H1, followed by H0, which represent the two fuel-cell electric configurations with the lowest range and seating capacity.

Differences in passenger- and aircraft-to-flight assignments lead to changes in network topology as well. Average degree increases by +4-5 %, indicating a noticeable enhancement in average connectivity. This is further supported by a +3 % increase in average flow betweenness. Additionally, average eigenvector centrality shows an increase correlated with the size of the aircraft, with up to +1.6 % growth. This suggests that the average importance of nodes increases with the capability of the hydrogen aircraft configuration, while H0 does not alter the network substantially in this regard. Similarly, closeness centrality exhibits a more moderate increase of up to +0.3 %, indicating a slightly lower average mean distance between nodes for more capable configurations.

5.4. Analysis of node groups

Examining deviations among node groups (see Fig. 9) provides insights into how nodes with varying characteristics are influenced differently by the introduction of a hydrogen aircraft. A notable difference emerges for airports with and without LH_2-supply (refer to Section 3.4 for selection of LH_2 supply). Nodes with hydrogen supply experience a greater increase in centrality compared to those without. Moreover, this disparity diminishes as the aircraft size and range increase. This trend is particularly evident for eigenvector centrality, as well as for node degree and flow betweenness. Specifically, eigenvector centrality, an indicator of node importance increases by approximately +5 % for nodes with hydrogen supply, while it decreases for nodes without hydrogen supply by -9 to -15 %. This difference is especially pronounced for scenarios involving hydrogen fuel cell configurations (H0 & H1), where nodes with hydrogen supply substantially increase their importance. For node degree and flow betweenness, the gap decreases from 2-3 p.p. to roughly 0.4 p.p. between H0 and $H2^B$. Although closeness shows the lowest average change between the standard and hydrogen scenarios, it still increases by an average of +0.3 p.p. more at hydrogen supplied nodes. In summary, it can be concluded that nodes with LH_2 supply experience a greater increase in connectivity within the network compared to those without, and this effect is more pronounced configurations with lower range/capacity.

Notable differences can furthermore be observed comparing topology changes of already highly connected (top-50 in terms of degree) against the system-level characteristics. On a relative level, the topology indicators grow less for all hydrogen configuration introductions than on a system level. Average degree for example grows by +4-4.5 % on a system level, while only increasing by +1.7-2.3 % for the top-50 nodes. Due to the higher baseline, the absolute gain is still higher for the top-50 nodes, at +2.1-3.1 compared to +1.0-1.1 on system level. While this could be a result of the defined threshold of 26 flights p.a. that is increasingly met with the introduction of smaller aircraft, it shows a qualitative trend of hydrogen aircraft enabling smaller nodes to economically establish more frequent connections. This is supported by the development of eigenvector centrality, as well as flow betweenness, which both grow less on relative and absolute terms for the top-50 nodes. Especially H0, but also $H1^+$ & $H2^A$ show a notable difference for relevant centrality indicators on system level compared to the top-50 nodes. This dynamic will be called decentralization of the network.

5.5. Discussion of results for H1

To examine the network changes more granularly, the hydrogen introduction with the highest network disruption, H1, is examined more closely. H1 represents the 140 seat, 2,000 km range fuel-cell electric aircraft. Observing the fleet development, the introduction of H1 forces the retirement of all remaining B737MAX7, A220, A330neo, and 60 % of the 120-seat narrowbody-HECA aircraft. H1 hence replaces aircraft of comparable size while phasing out larger, less efficient aircraft, allowing more efficient ones to cover longer routes. H1 also captures 27 % of ground transportation ASKs due to its favourable economics for distances over 300 km. This results in H1 comprising 34 % of the overall fleet in Europe, decreasing the average seating capacity per aircraft substantially and requiring more aircraft and flights to meet the same demand.

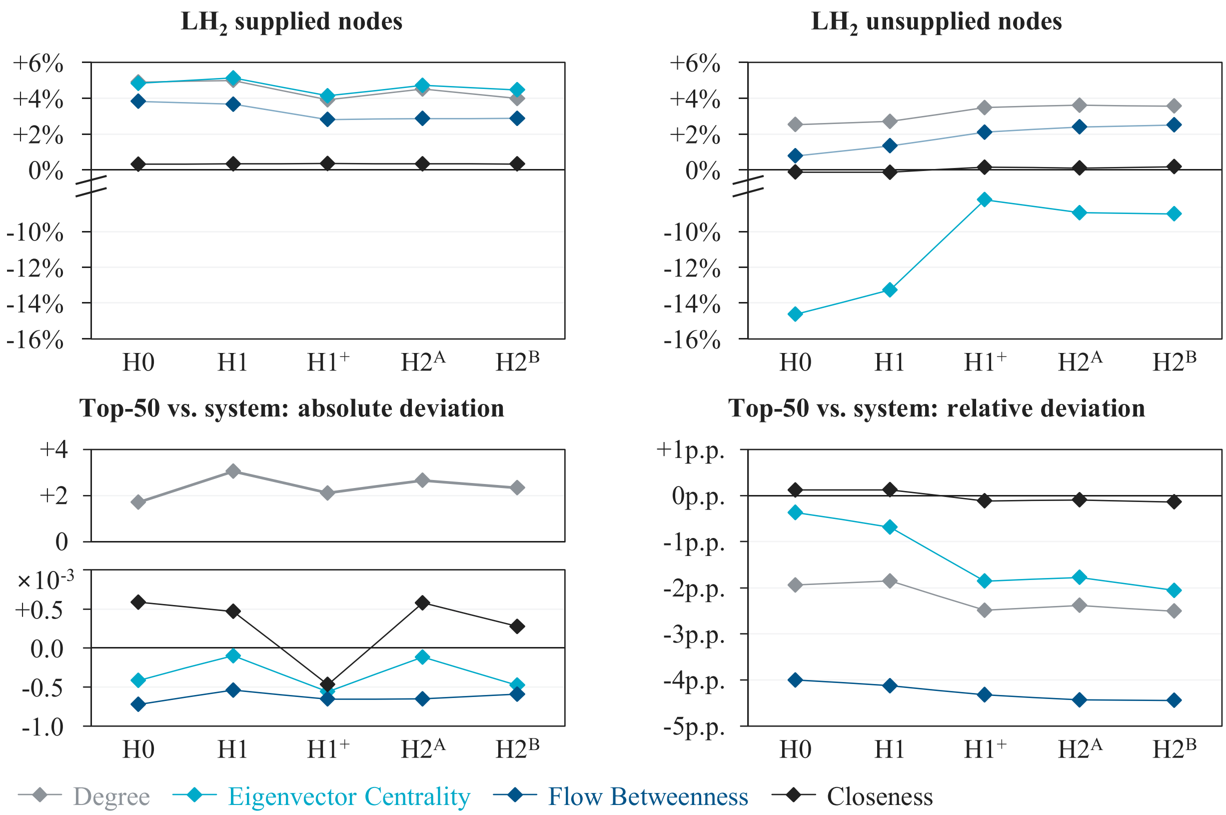

Fig. 9. Difference in topology indicators between node groups.

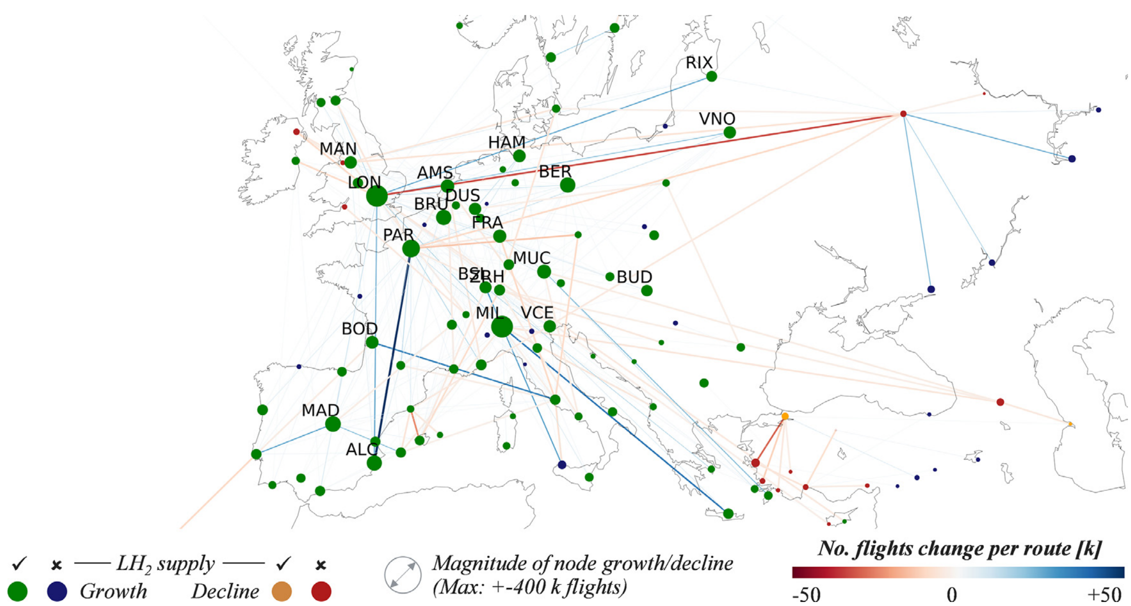

Fig. 10. Intra-European flight network development resulting from introduction of H1 (top-300 routes depicted, top-20 airports annotated, measured in absolute change).

Fig. 10 illustrates the changes in number of flights per route and airport when deploying H1 compared to the standard scenario. Notably, major nodes with hydrogen supply experience a growth in flight movements, while others without hydrogen supply, like MOW, TBS or IZM, see a decline in flight volumes. Stations with hydrogen supply nearby absorb stopover volumes from these nodes, like RIX or VNO for MOW. Airports with capacity constraints such as VIE or DUB witness a decrease in passenger volume (-12 to -15 %). Overall, 14 metropolitan-area nodes reach their capacity limit, with six more approaching it closely (>92 % of capacity limit, most notably including LON, PAR & FRA). A topographical illustration of passenger and flight changes for all other configurations can be found in Figs. 15 and 16 in Appendix A.7.

Fig. 11 shows the station-wise development of flights and stopover passenger volumes with the introduction of H1, as function of the local LH_2 price. Especially flight movements show a negative correlation with LH_2 price if the station is not capacity constrained before. In terms

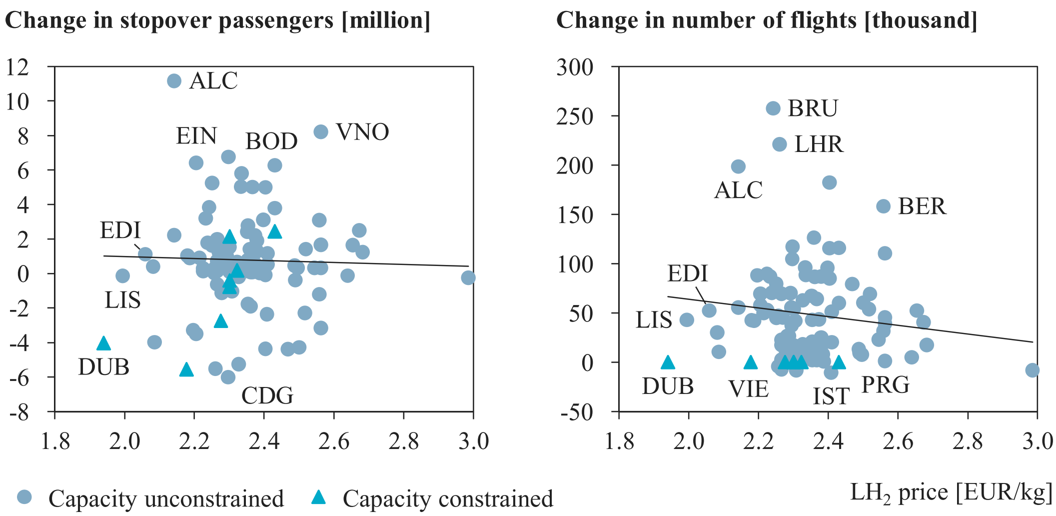

Fig. 11. Change in stopover passenger and flight volumes after introduction of H1 depending on local LH_2 price and airport capacities (only hydrogen-supplied airports).

of stopover passengers, the correlation is less evident. This can be explained by the large share of passenger volumes to and from outside of Europe, for which H1 is not a viable option, and hence hydrogen price is less relevant. It can however be observed that capacity constrained airports lose stopover passenger volume with the introduction of hydrogen aircraft, as a result of new, more economic options being available at airports with hydrogen supply. The three stations with highest stopover volume increase, ALC, BSL and RIX, are characterized by hydrogen supply, sufficient growth potential, and a geographically favourable location as stopover for extra-European routes. ALC for example shows a relatively low LH_2 price, is located close to North Africa, and within the H1 range of many stations in North/Central Europe. A similar dynamic is evident for RIX/VNO for routes to Eastern Asia, which leads to a much more economically attractive option as stopover than MOW which has no hydrogen supply. Both examples represent a favourable hydrogen replacement for nodes that are capacity constrained (BCN) or without hydrogen supply (MOW). Although different in quantity, the described dynamics can be qualitatively observed across all different hydrogen aircraft configurations.

5.6. Alternative scenarios

Four different alternative scenarios deviating from the standard parameters are examined in detail in this Section, before discussing four further sensitivity analyses on a high level. It is emphasized that although these scenarios are investigated in isolation, it is possible for a combination of multiple scenarios to develop, with varying influence of each of the considered variables.

The first main alternative scenario (AS1) investigates a world in which more battery-electric aircraft are available within Europe, namely 1,525 aircraft instead of only 525. This simulates a considerable uptake in regional aircraft adoption compared to the current network based on the increased economical benefits of battery-electric aircraft and reflects a potential stimulation of the regional aircraft market following the introduction of novel aircraft technology (Henke et al. 2010; Grimme et al. 2020). The second (AS2) introduces the process of tankering. Tankering refers to the practice of carrying more fuel than required for the planned flight to avoid refuelling at the destination airport. Operators make use of this strategy if fuel prices between airports differ substantially. Next to fuel price differences, following this strategy can be even more beneficial for hydrogen than for conventional aircraft since the additional weight penalties are much less severe (Huete et al. 2022). Moreover, the lack of hydrogen supply at certain stations, especially in the early phases, of the hydrogen adoption process makes tankering essential to integrate these stations (Wiener et al. 2023). For this scenario, hydrogen aircraft can reach airports that do not have hydrogen supply if the route distance does not exceed half of the respective aircraft range. The second change is that for all routes, the lower hydrogen price of both airports is used for both legs. The third alternative scenario (AS3) simulates a relaxation of airport capacity constraints by +50 %. This hypothetical scenario explores a world in which airport capacity constraints are overcome, partly as a result of increased public acceptance towards airport extensions. This is especially interesting as quantifying the influence of airport constraints may add value to a potential discussion about airport extensions in favour of increased sustainability. Finally, the last alternative scenario (AS4) investigates jet fuel/SAF mix price reduction of -15 %. This projects a development in which the ETS price is lower than expected and/or production costs of PtL SAF are substantially reduced. This reflects the circumstance that fuel and emissions price development is highly uncertain while being central to the adoption of hydrogen aviation.

Fig. 12 illustrates the resulting changes for all of the four scenarios. It shows the absolute deviation in changes to various model parameters induced by the introduction of the corresponding hydrogen aircraft configuration. It is important to note that the baseline of the percentage-change is different for each scenario.

In general, the deviation remains below ±5p.p., indicating a robust standard scenario. Direct operating costs deviation only increases for AS4 (+1p.p), as the relative cost of deploying hydrogen aircraft increases. Higher CO_2 emission savings can only be achieved in AS2 with tankering. All other scenarios have a weakening effect on CO_2 emissions reduction. Deviation in number of flights and aircraft deployed increases with AS1 & AS3, while it decreases with AS4. As the impact on network topology in all alternative scenarios is limited, the discussion will be limited to measures depicted in Fig. 12.

Increasing the number of available 75-seat, 1,000 km-range battery-electric aircraft within Europe to 1,525 instead of 525 (AS1) results in a notable rise in both the number of flights and aircraft, even without the introduction of hydrogen aircraft. The system-level number of flights increase by +6 %, and the number of deployed aircraft increase by +4 % (equivalent to +586 aircraft), indicating considerable strain on flight movements. CO_2 emissions savings on system level sum up to -2 % (-7 $MtCO_2$). Despite the heightened pressure on airport capacities, the overall changes induced by the introduction of hydrogen aircraft are similar to the standard scenario. This observation reinforces the importance of introducing narrowbody hydrogen aircraft additional to battery-electric

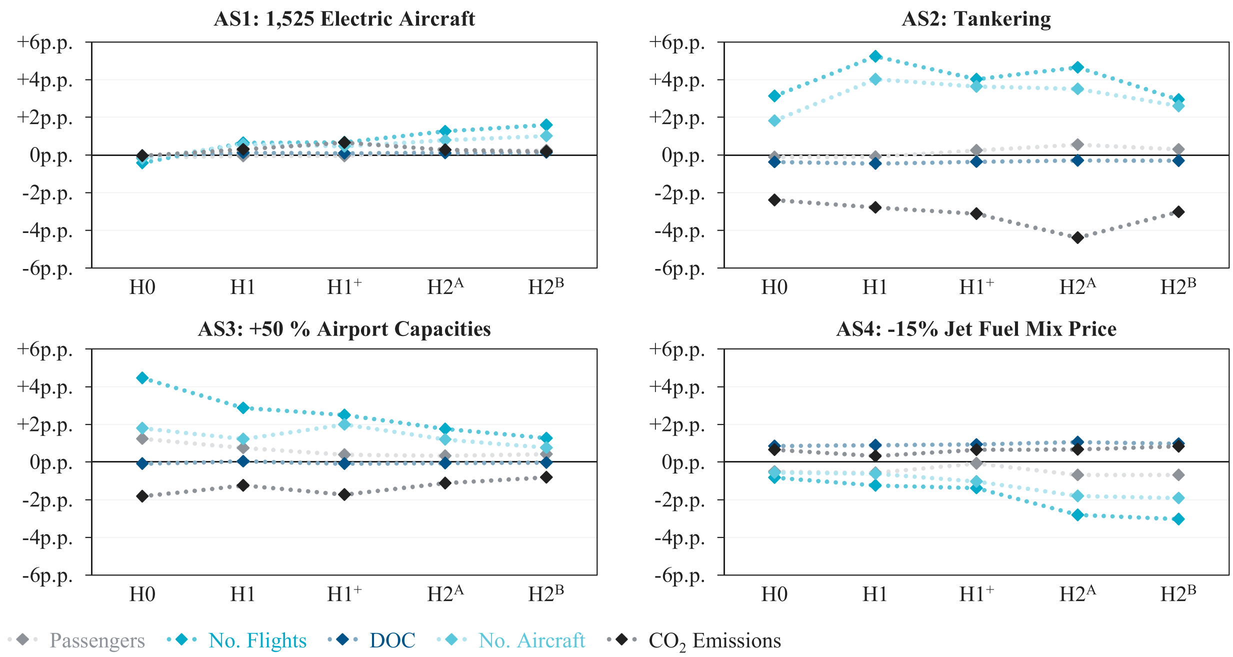

Fig. 12. Deviation of parameter changes for alternative scenarios compared to the standard scenario.

regional aircraft. The hypothesis is further supported by a relatively minimal deviation in changes for AS1, except for mitigating CO_2 emissions reduction of $H1^+$ by 0.7 p.p. on system-level. A counterintuitive finding is the higher increase in flights and aircraft for $H2^A$ & $H2^B$ compared to the standard scenario, while H0 even shows a lower increase in flights and aircraft. This trend emerges from higher-capacity hydrogen aircraft replacing a greater number of widebody than narrowbody aircraft compared to the standard scenario, as electric aircraft already cover the lower-capacity & -range segment.

Introducing a tankering option (AS2) brings several interesting changes to the network. The CO_2 emissions reduction is enhanced by between -2 to -4 p.p. as hydrogen aircraft can be deployed on more routes. Especially the potential of $H2^A$ is enhanced, potentially as a result of the highest design range and the potential to cover the most additional routes. It however requires 6,154 aircraft to reach this level of emissions reduction, the highest number of hydrogen aircraft for all scenarios. Since the lower LH_2 price of any two connected stations can be leveraged, direct operating costs are lowered. Especially the fuel cell electric variant H1 shows an additional cost reduction by -0.5 p.p. Number of aircraft and flights however increase even more than in the standard scenario, by +3 to +5 p.p. This means an increase of +21 % in flight movements for H0, which would strain the air transportation system considerably. Overall, tankering represents a good opportunity to leverage the advantages of hydrogen in the beginning, but additional emissions and cost gains also imply a high number of flights and aircraft required.

Increasing assumed airport movement capacities by +50 % (AS3) also shows an elevated level of changes in the impact hydrogen aircraft have on the network. Number of aircraft and flights would increase substantially more than in the standard scenario (+1-5 p.p.), as the network has more leeway to grow using the most efficient routes and airports. This also has a positive impact on direct operating costs, decreasing by up to -0.1 p.p. As expected, this dynamic is dampened by increasing capabilities of the aircraft, as less additional flights and aircraft are required for configurations with more seats and range.

The impact of a -15 % reduced jet fuel mix price (AS4) can be observed mainly on system-level direct operating costs, decreasing by -5 % in the baseline (without hydrogen aircraft). At the same time, CO_2 emissions increase by +0.4 % as the penalty for burning jet fuel is lower. Accordingly, the impact of introducing hydrogen aircraft has a lower effect on DOC and CO_2 emissions reduction, since the economic parity point is shifted in favour of conventional aircraft types (+0.3 to +1.0 p.p.). Number of flights and aircraft are also increasing less than in the standard scenario. Notably, this effect is increasing for higher range/capacity configurations by up to -3 p.p. for $H2^B$ as the impact of fuel prices is higher for longer-range routes.

As a last step, four additional sensitivities are qualitatively discussed in less detail (see Fig. 13). These serve to quantify the effect on the result if key assumptions are modified. The first sensitivity simulates a reduction of available hydrogen aircraft due to production bottlenecks to 2,750, implying a monthly production rate of 25 aircraft over ten years (with eleven productive months). The same effect could emerge if EIS is delayed by five years to 2040. Not surprisingly, this approximately halves the effect of introducing hydrogen aircraft on all levels, including CO_2 emissions reduction, flights & aircraft increase, as well as topology indicators. It can be concluded that a high number of hydrogen aircraft (>5,000) needs to be produced within the aspired time frame in order to leverage the emissions reduction potential.

A similar result evolves when limiting the number of airports that offer hydrogen supply based on the assumption that, especially in the beginning, not all airports will have built up a green hydrogen value chain. A limitation of the hydrogen supply to the top-30 airports by movements in 2019 dampens the emissions reduction to -6 % at best (using $H1^+$ or $H2^A$). Since a large share of demand occurs at these airports, the dampening effect would be even higher if the same number of other, smaller airports would only have LH_2 supply instead of the top-30. The effect is however mitigated when enabling tankering. This combined scenario (tankering + top-30 nodes with LH_2 supply) achieves only -2.5-7 p.p. less emissions reduction than the standard scenario. Especially the impact of $H2^A$ is similar to the standard scenario, while the impact of H0 is substantially reduced.

The fourth scenario excludes the use of ground transportation both with and without hydrogen aircraft to investigate the role of modal shift. In this scenario, the number of aircraft required to service ground trans-

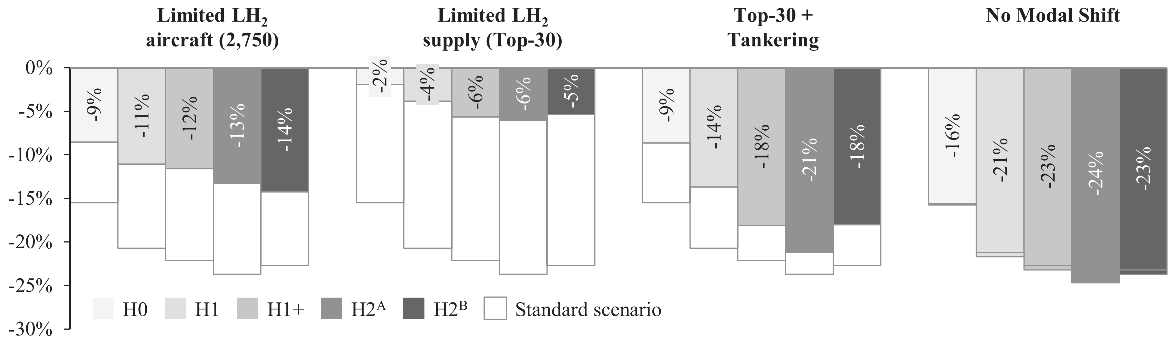

Fig. 13. CO_2 emissions reduction by aircraft type and sensitivity analysis.

portation routes are increased but the additional number of flight movements induced by the introduction of hydrogen aircraft are reduced. This is a result of the high number of flights required without hydrogen aircraft already to service the low-distance routes previously covered by ground transportation. CO_2 emissions would be both on a higher level in general, but also be less impacted by the introduction of hydrogen aircraft. The replacement of short routes with zero-emissions transportation can therefore even be seen beneficial to leverage the potential of hydrogen aircraft on longer, more polluting routes.

6. Conclusion and outlook

The aim of this study was to investigate the impact of introducing first-generation narrowbody hydrogen aircraft on the passenger air transportation network in Europe. To achieve this, a network model was developed based on the 2019 air transportation network, utilizing complex network modelling and linear optimization techniques. The results of this analysis can be summarized into three main findings.

First, the study demonstrated the feasibility of reconstructing the passenger air transportation network by minimizing direct operating costs without considering airline-specific factors or revenue/air fares. The model was able to explain 93 % of the variation in passenger volumes per origin-destination pair within Europe and >96 % of the variation in relevant centrality measures, including degree, eigenvector, and flow betweenness centrality. This finding is compelling from two different perspectives. First, it represents a novel, simple, and holistic approach to describing the air transportation network, which could have applications beyond the scope of this study. Second, despite airlines aiming for their local cost optimum within their path-dependent operational constraints (e.g., available fleet), competition amongst airlines appears to drive their actions towards a global optimum. This observation is supported by the relatively low profitability that most airlines achieve (IATA 2020b).

The second finding revealed that the introduction of first-generation narrowbody hydrogen aircraft will have a considerable impact on the air transportation network, contingent upon the aircraft design in terms of seating capacity and range. With low capacity and range, flight volumes will increase substantially, intensifying strains on airport capacities and airspace, potentially leading to heightened congestion and delays. Simultaneously, this surge in flights would enhance average connectivity and decentralization of the system. Consequently, the introduction of hydrogen-powered aircraft not only contributes positively to emissions reduction, but also enhances passenger connectivity. However, achieving a large hydrogen fleet of appr. 5,000 aircraft by 2050 demands considerable efforts in aircraft development, production ramp-up, and accelerated retirement of the existing fleet – all of which is based on the premise of competitive operating costs compared to conventional propulsion. This underlines the need for concerted efforts from policymakers to incentivize the transition towards hydrogen aviation and from industry to advance technological and infrastructural development.

Third, the study also showed that nodes with hydrogen supply benefit from the introduction of hydrogen aircraft, particularly in terms of flight movements. This effect is especially notable for airports near major hubs that are either capacity-constrained or lack favourable supply of LH_2. This presents an opportunity for smaller airports with favourable LH_2 supply to invest in hydrogen infrastructure. However, no correlation was found between the specific LH_2 price at the dispenser and increase in stopover volumes. This could be attributed to the relatively low share of fuel cost on short-to-medium distance routes, for which hydrogen aircraft designs in this study have been limited to. Nonetheless, this dynamic could shift with the introduction of potential long-haul hydrogen combustion aircraft.

Based on the outlined limitations of the modelling methodology, future research could enhance the model by

- including air fares to enable optimization of system profit,
- assessing airline-specific externalities to increase model fit,
- including supply-demand interactions,
- enhancing hydrogen aircraft performance characteristics including advanced aircraft design modelling, and
- extending the model scope to include other regions or aircraft configurations.

Declaration of interests

The authors declare the following financial interests/personal relationships which may be considered as potential competing interests:

Alexander Rau reports financial support, administrative support, travel, and writing assistance were provided by Roland Berger GmbH. If there are other authors, they declare that they have no known competing financial interests or personal relationships that could have appeared to influence the work reported in this paper.

CRediT authorship contribution statement

Alexander Rau: Writing – review & editing, Writing – original draft, Visualization, Validation, Software, Resources, Project administration, Methodology, Investigation, Formal analysis, Data curation, Conceptualization. **Eike Stumpf:** Writing – review & editing, Validation, Supervision. **Marc Gelhausen:** Writing – review & editing, Validation.

Acknowledgements

During the preparation of this work the authors used ChatGPT 3.5 in order to improve readability and language. After using this tool/service, the authors reviewed and edited the content as needed and take full responsibility for the content of the publication.

Appendix

A.1. Abbreviations

Table 4
Abbreviations.

Abbr.	Explanation	Abbr.	Explanation
°C	Degree Celsius	MAE	Mean Absolute Error
ASK	Available Seat Kilometer	MIDT	Marketing Information Data Transfer
bn	billion	MILP	Mixed Integer Linear Programming
ceo	Classic Engine Option	MRO	Maintenance Repair & Overhaul
CO_2	Carbon Dioxide	Mt	Megatons
DLR	German Aerospace Center	MTOW	Maximum Take-off Weight
DOC	Direct Operating Cost	NB	Narrowbody
EIS	Entry-Into-Service date	neo	New Engine Option
etc.	et cetera	NO_X	Nitrogen Oxide
ETS	Emissions Trading Scheme	OD	Origin-Destination
GDP	Gross Domestic Product	OEW	Operating Empty weight
h	hour	p.p.	Percentage points
HECA	Hyper Efficient Conventional Aircraft	PR	Production Rate
IATA	International Air Transport Association	PtL	Power-to-Liquid
ILR	Institute of Aerospace Systems, RWTH Aachen University	R^2	Coefficient of Determination
K	Kelvin	RPK	Revenue Passenger Kilometer
k	Thousand	SAF	Sustainable Aviation Fuel
kg	kilogram	SK	Seat Kilometer
km	Kilometer	t	metric tons
kW	kiloWatt	tn	trillion
kWh	kilo Watt hours	WB	Widebody
LH_2	Liquid Hydrogen	XLR	Extra Long Range
m	Million		

A.2. Network analysis

Table 5
Network analysis metrics.

Category	Explanation	Variable	Formula	Further information	Source
Degree	Number of links connected to a node i	d_i	$\sum_{j=1}^{N} a_{ij}$	a_{ij} is the value of link ij in the adjacency matrix	Sallan and Lordan (2020)
Degree distribution	Provides information about the connectivity distribution across the network	$P(d)$	$\frac{N_d}{N}$	N_d is the number of nodes with degree d	
Cumulative degree distribution		$P_{cum}(d)$	$\sum_{k'=k}^{\infty} P(d')$		
Betweenness centrality	Ability of a node to stand between two others. Measures the likelihood of being on the shortest path between two unconnected nodes.	$C_b(i)$	$\sum_{j \neq g \neq i \epsilon N} \frac{\sigma_{jg}(i)}{\sigma_{jg}}$	σ_{jg} represents the number of shortest paths between j and g passing through i, for $j, g \epsilon N$	Freeman (1977), Guimerà et al. (2005)
Flow Betweenness	Weighted betweenness centrality based on passenger flows. Conceptualizes system as electrical network with links as resistors, and nodes as junctions connecting the resistors. The significance of a node's flow betweenness is linked to the volume of "current" traversing through it.	$F_b(i)$	$\sum_{j \neq g \neq i \epsilon N} \tau_{jg}(i)$	$\tau_{jg}(i)$ is the passenger flow through node i between origin j and destination g	Cheung et al. (2020)
Closeness centrality	Measures the "accessibility" or proximity of a node in a network.	$C_c(i)$	$\frac{N-1}{\sum_{j \epsilon N_{j \neq i}} Dist(i,j)}$	$Dist(i, j)$ is the aggregated path distance	Newman (2005), Malighetti et al. (2008)
Eigenvector centrality	Importance of a node by incorporating the importance of its connected neighbors.	$C_E(i)$	$\frac{1}{\lambda} \sum_{j} W_{ij} C_E(j)$	$\lambda \neq 0$ is the largest eigenvalue, W is the passenger flow matrix	Cheung et al. (2020)

A.3. Fleet forecast

Table 6
Production rates (PR) per year [#p.a.] for current aircraft types.

Aircraft type	2019 actuals[1]	PR target mid-2020s[2]	Assumed at base year[3]	End-of-prod.
A220	48	154 (14 p.m.)	140	2035
A319neo/A320neo	383	825 (75 p.m.) incl. A321neo	313	2035
A321neo	168		405	2040
A330neo	41	44 (4 p.m.)	43	2045
A350	112	99 (9 p.m.)	103	2040
ATR42/72	60	80	60	>2050
B737 MAX7-9	57	575 (50 p.m.) incl. MAX10	411	2035
B777	45	46 (4 p.m.)	45 (777X)	2025
B787	158	115 (10 p.m.)	102	2040
E175	67	100 incl. E190/95	35	2030
E190/95 E2	14		46	2035
Other Jet	63	-	118	>2050
Turboprop	25	-	46	2030

[1] Based on TEAL 2023.
[2] Based on Airbus 5/27/2021, 7/26/2023; ATR 3/30/2023; Aviation Week 6/12/2023; Boeing 2023; assuming a 11-month production period per year at Airbus, and 11.5 month at Boeing.
[3] Base year = 2026; Based on TEAL 2023; PR = Production rate p.a.

Table 7
New aircraft type EIS assumptions until 2050[1].

Aircraft type	Seat capacity	PR at base year[12]	EIS	Range [km]	Reference aircraft
B777X	400	45	2025	16,000	-
A321XLR	206	50	2024	8,300	-
B737 MAX10	204	158	2024	6,100	-
E-Aircraft	75	75	2030	1,000	ATR72
Narrow-body HECA	90	36	2040	3,000	E170/75 E2
	120	46	2040	4,000	E190/95 E2
	150	98	2040	5,000	A319neo
	170	211	2035	7,000	B737MAX7
	180	427	2035	6,000	B737MAX8
	200	204	2045	8,500	A321XLR
	235	408	2045	6,500	A321neo
Widebody HECA	320	266	2040	16,000	A350-900
	400	72	2045	15,000	B777X

[1] Reference aircraft is the aircraft which the new generation replaces, and of which modified specifications are based on. Change in specifications include MTOW, OEW, Thrust, and Engine weight; PR = Production Rate HECA = Hyper-efficient conventional aircraft (next-generation turbo-engine).

A.4. Direct Operating Costs

Table 8
Calculation formula for DOC building blocks.

Category	Explanation	Variable	Formula
Utilization	Flight cycles per year	FC	$\frac{OT_{p.a.}}{FT+BTS_{adj}} = \frac{POT_{p.a.}-DT_{p.a.}}{FT+BTS(FT)}$
Utilization	Block time supplement	$BTS(FT)$	$1.83 + \begin{cases} -0.1h, & FT < 4h \\ FT - 4.1h, & 4h \leq FT < 5.7h \\ 1.5h, & FT \geq 5.7h \end{cases}$
Fuel	Fuel cost	DOC_{fuel}	$TF \cdot P_{fuel} \cdot FC$
Fees	Fees	DOC_{fees}	$DOC_{ldg} + DOC_{gr} + DOC_{nav}$
Fees	Landing fees	DOC_{ldg}	$K_{ldg} \cdot MTOW \cdot FC$
Fees	Ground handling fees	DOC_{gr}	$K_{gr} \cdot PL \cdot FC$
Fees	Navigation fees	DOC_{nav}	$K_{nav} \cdot D/100 \cdot \sqrt{\frac{MTOW}{50{,}000}} \cdot FC$
Fees	Payload	PL	$PL_{pax} + PL_{Cargo}$
Fees	Passenger payload	PL_{pax}	$n_{seats} \cdot LF_{pax} \cdot PL_{single\ pax}$
Fees	Cargo payload	PL_{Cargo}	$LF_{Cargo} \cdot (MTOW - OEW - BF - PL_{pax})$
Fees	Block fuel[1]	BF	$TF \cdot 1.1$
Maintenance	Maintenance costs	$DOC_{maint.}$	$DOC_{AF,mat} + DOC_{AF,per} + DOC_{ENG}$
Maintenance	Airframe material	$DOC_{AF,mat}$	$(OEW \cdot (0.21 \cdot FT + 13.7) + 57.5) \cdot FC$
Maintenance	Airframe personnel	$DOC_{AF,per}$	$LR \cdot (1 + B) \cdot [(0.655 + 0.01 \cdot OEW) \cdot FT + 0.254 + 0.02 \cdot OEW] \cdot FC$
Maintenance	Engine maintenance	DOC_{ENG}	$(N_{ENG} \cdot (1.5 \cdot SLST + 30.5 \cdot FT + 10.6)) \cdot FC$
Crew	Crew cost	DOC_{crew}	$CC \cdot (S_{FA} \cdot n_{FA} \cdot n_{seats} + S_{FC})$
Capital	Capital cost	DOC_{cap}	$(P_{OEW} \cdot (OWE - W_{ENG} \cdot N_{ENG}) + P_{ENG} \cdot W_{ENG} \cdot N_{ENG})) \cdot (a + f_{ins})$
Capital	Annuity rate	a	$IR \cdot \frac{1-f_{RV} \cdot (\frac{1}{1+IR})^{DP}}{1-(\frac{1}{1+IR})^{DP}}$

[1] Includes +10% of the required trip fuel for contingency & holding/diversion, see Janovec et al. 2023.

Table 9
Assumptions for direct operating costs.

Category	Explanation	Variable	Unit	Assumption	Source
Utilization	Operating time p.a.	$OT_{p.a.}$	h	*var*	Scholz, Thorbeck (2013)
Utilization	Potential operating time p.a.	$POT_{p.a.}$	h	$365 \cdot 24 = 8760$	
Utilization	Forced downtime p.a.	$DT_{p.a.}$	h	2748.8	
Utilization	Flight time	FT	h	*var*	European Environment Agency (2019)
Fuel	Trip fuel	TF	kWh	*var*	
Fuel	Fuel unit cost	P_{fuel}	$€_{2019}$/kWh	*var*	Network model
Fuel	Energy factor LH_2	f_{LH2}	$\frac{kg_{JetFuel}}{kWh} / \frac{kg_{H_2}}{kWh}$	*2.78*	Adler and Martins (2023)
Fuel	Energy factor El.	f_{EL}	$\frac{kg_{JetFuel}}{kWh} / \frac{kg_{EL}}{kWh}$	*0.33*	Hospodka (2021)
Fees	Landing fee coefficient	K_{ldg}	$€_{2010}$/kg	*0.01*	Scholz, Thorbeck (2013)
Fees	Maximum take-off weight	$MTOW$	kg	*var*	Fleet model
Fees	Operating empty weight	OEW	kg	*var*	
Fees	Ground handling fee rate	K_{ldg}	$€_{2010}$/kg	*0.1*	Scholz, Thorbeck (2013)
Fees	Belly cargo load factor	LF_{Cargo}	-	*0.4*	Mota et al. (2017), IATA (2020b, p. 33)
Fees	Number of seats	n_{seats}	-	*var*	Fleet model
Fees	Passenger load factor	LF_{pax}	-	*0.826*	IATA (2020a)
Fees	Passenger weight incl. luggage	$PL_{single\ pax}$	kg	*100*	Scholz, Thorbeck (2013)
Fees	Navigation unit rate	K_{nav}	$€_{2010}$/km	$\begin{cases} 100\ \forall D \leq 3,000 \\ 65\ \forall D > 3,000 \end{cases}$	Proprietary, based on Scholz, Thorbeck (2013)
Fees	Flight distance	D	km	*var*	Network model
Maintenance	Labor rate	LR	$€_{2010}$/h	*50*	Scholz, Thorbeck (2013)
Maintenance	Cost burden	B	-	*2*	
Maintenance	Number of engines	N_{ENG}	-	*var*	Network model
Maintenance	Sea level static thrust	$SLST$	kN	*var*	
Crew	Number of crews per aircraft	CC	-	*6*	Proprietary, based on Scholz, Thorbeck (2013)
Crew	Number of flight attendants per aircraft	n_{FA}	1/seats	*1/50*, $n_{FA} \cdot n_{seats} \in \mathbb{N}^+$	Scholz, Thorbeck (2013)
Crew	Average yearly salary of one flight attendant	S_{FA}	$€_{2010}$/year	*60,000*	
Crew	Average yearly salary of the cockpit crew	S_{FC}	$€_{2010}$/year	*300,000*	
Capital	Price per kg OEW	P_{OWE}	$€_{2010}$/kg	*1,150*	
Capital	Price per engine weight	P_{ENG}	$€_{2010}$/kg	*2,500*	
Capital	Insurance rate	f_{ins}	%	*0.5*	
Capital	Interest Rate	IR	%	*5*	
Capital	Share of the residual value of the aircraft price at sale	f_{RV}	%	*10*	
Capital	Depreciation rate	DP	years	*14*	
Capital	Engine weight	W_{ENG}	kg	*var*	Fleet model

A.5. Flight bundling

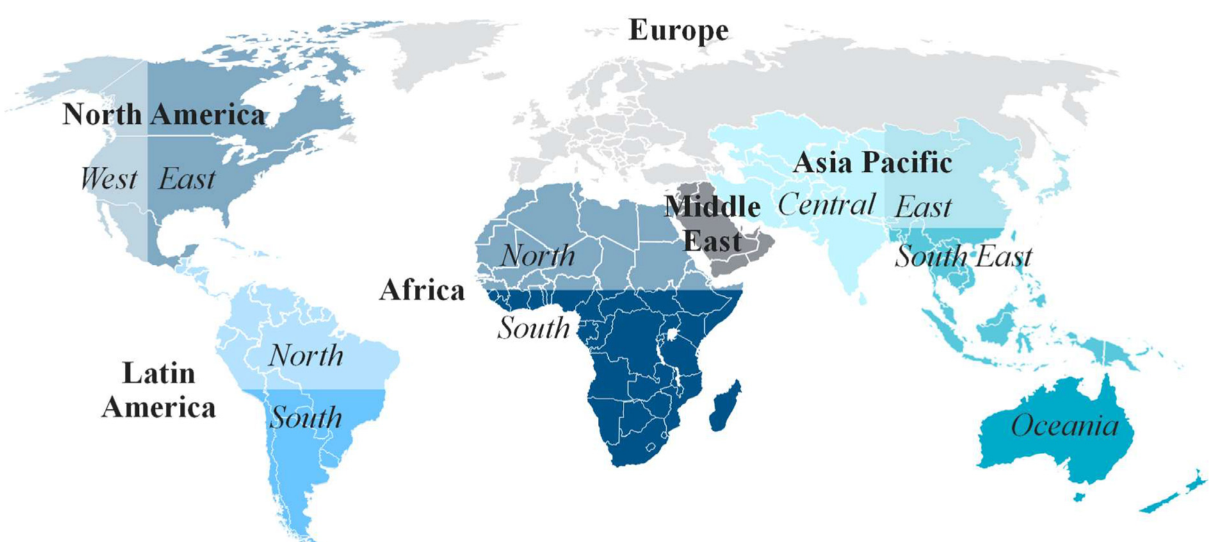

Fig. 14. Extra-European flight bundling by region.

A.6. Airport hub categorization

Table 10
Airport hub categorization.

Hub category	Explanation	IATA codes
Airline hubs	Primary and secondary hubs of all European full-service carriers. Can serve as stopover on all demand items.	AMS, ARN, ATH, CDG, CPH, DUB, FCO, FRA, HEL, IST, KBP, KEF, LGW, LHR, LIS, MAD, MUC, SVO, VIE, WAW, ZRH
Intra-European hubs	Top 50 airports (excl. airline hubs) by movements in 2019. Can serve as stopover on intra-European demand items.	ADB, AGP, ALC, ALG, AYT, BCN, BER, BGO, BGY, BHX, BLQ, BRU, BSL, BUD, CGN, CTA, DME, DUS, EDI, ESB, GLA, GVA, HAM, KBP, LCY, LED, LGW, LIN, LPA, LTN, LYS, MAN, MRS, MXP, NAP, NCE, OPO, ORY, OSL, OTP, PMI, PRG, RIX, SAW, STN, STR, TFN, TLS, VCE, VKO
Extra-European hubs	Airports that show higher extra-European passenger volume than demand in 2019. Can serve as stopover on extra-European demand items.	BEG, BUH, CGN, GYD, HAJ, LEJ, OVB, PRG, SVX, TBS, VVO, ZAG
Hydrogen hubs	Airports that are expected to have hydrogen supply by 2050 in the standard scenario (based on Wiener et al. 2023; Hoelzen et al. 2023, see Section 3.4). Can serve as stopover on all demand items in the hydrogen EIS scenarios.	AAL, ABZ, AGP, ALC, BCN, BER, BGO, BGY, BHX, BIA, BIO, BLL, BLQ, BOD, BOO, BRE, BRI, BRU, BSL, BUD, CAG, CHQ, CTA, DBV, DRS, DUS, EDI, EIN, EVN, FAO, FNC, GLA, GOT, GRO, GRZ, GVA, HAM, HER, IBZ, JMK, JTR, KGS, KRK, LCA, LGW, LIN, LTN, LYS, MAH, MAN, MLA, MMX, MRS, MXP, NAP, NCE, OLB, OPO, ORY, OSL, OTP, PMI, PUY, RHO, RIX, RJK, SCQ, SJJ, SKG, SOF, SPU, STN, STR, SVG, SVQ, SZG, TIA, TLL, TLS, TOS, TRD, TRF, VCE, VLC, VNO, ZAD

A.7. Hydrogen aircraft EIS assumptions

The **operating empty weight (OEW)** of hydrogen aircraft is increasing compared to the conventional aircraft due to additional weight of the cryogenic storage system and its integration in the fuselage. Hoelzen et al. (2022, p. 3114) assumes an operating empty weight increase by +20 % for a short-range and 25.7 % for a medium-range design. However, the **maximum take-off weight ($MTOW$)** only increases by 4.6 % and 2.3 %, respectively, since the total fuel mass is lower while passenger payload remains constant. The concepts in a study by Mukhopadhaya and Rutherford (2022) also show an increased OEW by +32 % for the turboprop version and +26 % for the narrowbody jet version, both assuming a tank gravimetric index of 35 %. MTOW for these concepts increases by +10 % for the turboprop design and decreases by -3 % for the narrowbody design. Verstraete (2009) assumes a -25 % MTOW reduction for a long-haul aircraft, while the Cryoplane study (Airbus Deutschland GmbH 2003, p. 3) assumes an increase of +23 % in OEW, while MTOW changes between +4.4 % and -14.8 %. Given the absence of a clear correlation with the range and capacity of the aircraft, the study will take the average increase in OEW of +24 % for all aircraft types and assume no change in MTOW, compared to the assigned parent type. Engine thrust and weight will therefore also not change as it is designed to meet the MTOW take-off requirements. These estimations concern hydrogen combustion aircraft. Very few studies exist for the weight implications of a fuel-cell powered electric aircraft, although a smaller hydrogen tank capacity can be assumed due to the higher energy efficiency (see below). The weight of the propulsion system itself depends heavily on the gravimetric power density of future fuel cell stacks, and is therefore subject to high uncertainty. Kadyk et al. (2018) estimate a -22 % decrease in overall weight of the energy system compared to current jet fuel aircraft if future light-weight, high-power fuel cell technology is realized. Accordingly, a -20 % weight discount is factored in for the fuel-cell technology aircraft types.

Specific energy usage (E_{req}) depends strongly on the tank gravimetric index. Adler and Martins (2023, p. 5) show that the specific energy usage compared to conventional jet fuel aircraft decreases with the gravimetric index and meets the jet fuel line at an index of approximately 55 %. Additionally, the delta above and below the “tipping point” increases with design range. The underlying reason is that beyond the “tipping point”, the specific energy advantage of hydrogen outweighs the drawbacks of increased aircraft weight due to the tank, and this effect increases with the amount of fuel being used. Hoelzen et al. (2022, p. 3114) estimate the specific energy usage to increase by +12 % for a short-range, and +18 % for a medium-range hydrogen combustion aircraft, using gravimetric indices of 40 % and 50 %, respectively. The authors explain the reduced energy efficiency due to increased drag from the longer fuselage, as well as the increased mass attributed to hydrogen tanks and the subsequent structural snowball effects. Mukhopadhaya and Rutherford (2022, p. 15) calculate an energy demand increase of +8-20 % for a 70-passenger turboprop and +13-36 % for a 165-passenger narrowbody aircraft, depending on the tank gravimetric efficiency, using 20 % on the lower end and 35 % on the higher end. Using high gravimetric indices, Verstraete (2013, p. 14824) and Janić (2014, p. 16435) both predict the fuel efficiency for a long-range combustion hydrogen aircraft to be -11 % lower than for a conventional long-range jet fuel aircraft. Lastly, the Cryoplane study (Airbus Deutschland GmbH 2003, p. 13) estimates specific energy consumption to change between +10 % and +9 % for a medium- and long-range aircraft up to +34 % for a business jet.

Again, these studies only consider hydrogen combustion technology. Studies on energy efficiency of aircraft using fuel cell electric propulsion are scarce, but further efficiencies can be expected when replacing the combustion engine with a fuel cell driven propeller. Even today, fuel cell stacks can achieve almost double the efficiency (~60 %) of a typical turboprop's thermal efficiency (25-30 %) (Adler and Martins 2023, p. 19; Bhatti et al. 2022, p. 11). This can mitigate the energy efficiency disadvantage of low gravimetric indices for short-range aircraft.

In line with existing research, this study will assume a gravimetric index of 40-50 % for the first-generation narrowbody hydrogen aircraft designs. This leads to a +12 % specific energy demand for hydrogen combustion designs for medium-range models. For short-range fuel-cell electric aircraft, the study will use a -5 % specific energy requirement, as a result of the higher propulsive efficiencies.

Capital costs (DOC_{cap}) are projected to be higher than comparable future jet fuel alternatives, mainly as a result of additional hydrogen storage integration. Hoelzen et al. (2022) expect +12-13 % increased capital expenditure for a combustion narrowbody aircraft without considering development efforts, mainly due to the cost and structural implications of integrating hydrogen tanks in the fuselage. Using a specific tank price of 550 $€_{2019}/kg_{LH2}$ and capacity of 3,500 kg for the short-range reference case (in line with Hoelzen et al. 2022), the additional costs for the hydrogen tank is estimated at +3-4 % of the total aircraft value. For a system using hydrogen fuel cells, Marksel and Brdnik (2023, p. 7) estimate the component costs at 151 $€_{2019}$/kW for the fuel cell and motor system of a 19-seat aircraft.[10] Using this assumption, the propulsion system cost for fuel cell

[10] Assuming 95 $€_{2019}$/kW for the electric motor, as well as 40 $€_{2019}$/kW and a ~60 % efficiency for the fuel cell system in the pessimistic case.

electric aircraft including the cryogenic storage could be ~30 % lower than for conventional aircraft.[11] However, there is no study yet comparing the economics of a scaled-up fuel cell aircraft design to meet the demands of transporting 130-140 people, especially given the high cost share of the hydrogen tanks. Therefore, capital costs are assumed to increase in line with Hoelzen et al. (2022) by 12 % for all aircraft types, independent of the operating empty weight.

Changes in **maintenance costs (DOC_{mc})** are categorized into airframe and engine costs. Airframe maintenance increases with operating empty weight, which is already accounted for given the increased aircraft mass due to the additional cryogenic storage system components and longer fuselage. This assumption is in line with the approach by Hoelzen et al. (2022), which is explained by the high uncertainty of estimating these costs given no prior studies regarding the topic.[12] Engine maintenance depends on the propulsion system. Janić (2014, p. 16433) expects maintenance efforts for the turbo-engine to decrease as a result of hydrogen as fuel exhibiting no impurities compared to jet fuel, potentially leading to an expected life time increase of +25 %. Since technological immaturities could have a counterbalancing effect for first-generation engines, no changes in engine maintenance efforts are conservatively assumed for this study. For the fuel cell-based propulsion system, maintenance efforts might decrease as oil changes and engine overhauls are not required. Marksel and Brdnik (2023, pp. 7–8) assume a considerable reduction in MRO efforts for a 19-seat hydrogen fuel cell aircraft. On the other hand, Hoff et al. (2023, p. 11) argue that MRO costs are not expected decrease, especially since the disassembly of the fuel cell stack for repair can be very costly. To remain on the conservative side, this study again does not assume any changes to engine maintenance for fuel cell systems. In summary, maintenance costs of hydrogen aircraft are subject to high uncertainty, but there is no evidence for a substantial increase additional to the higher efforts proportional to the operating weight of the aircraft.

A.8. Illustrative results

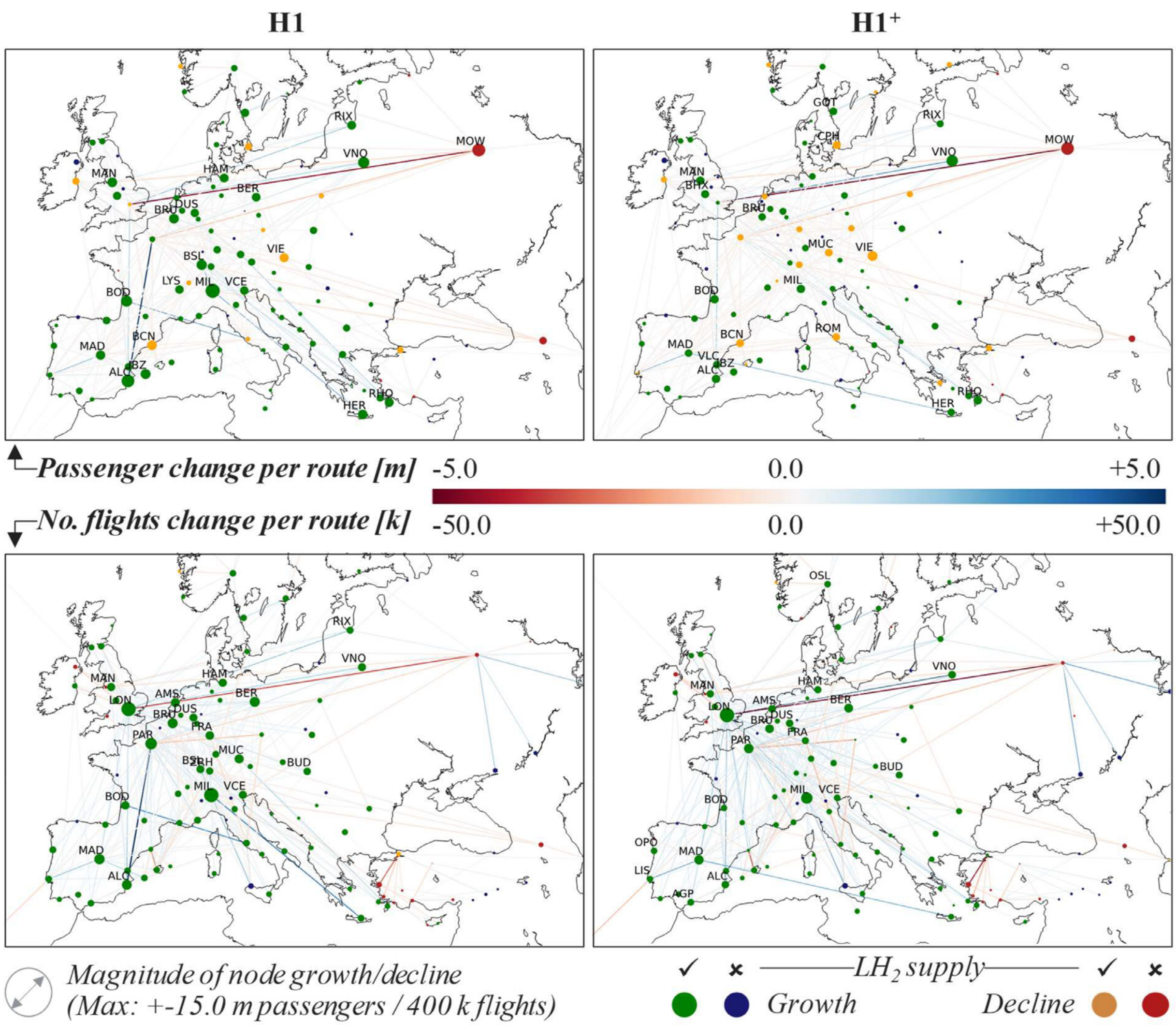

Fig. 15. Intra-European network development resulting from introduction of H1 & H1+ (top 300 routes, absolute change).

[11] Assuming a 19-seat aircraft comparable to DHC-6 Twin Otter with MTOW of 6,000 kg, peak power of 1,200 kW, engine weight of 260 kg and tank capacity of 1,200 $kg_{Jet\text{-}A}$ or 500 kg_{LH2}. With 2,500 $€_{2019}$/kg, the jet fuel version would cost 650,000 $€_{2019}$, while the fuel-cell version would be 181,200 $€_{2019}$ for the fuel cell system and 275,000 $€_{2019}$ for the hydrogen tanks (assuming 550 $€_{2019}/kg_{LH2}$).

[12] Meissner et al. 2023 analyze the maintenance costs of a hydrogen storage and distribution system, but only as an additional system for on-board power generation of a jet fuel-powered aircraft.

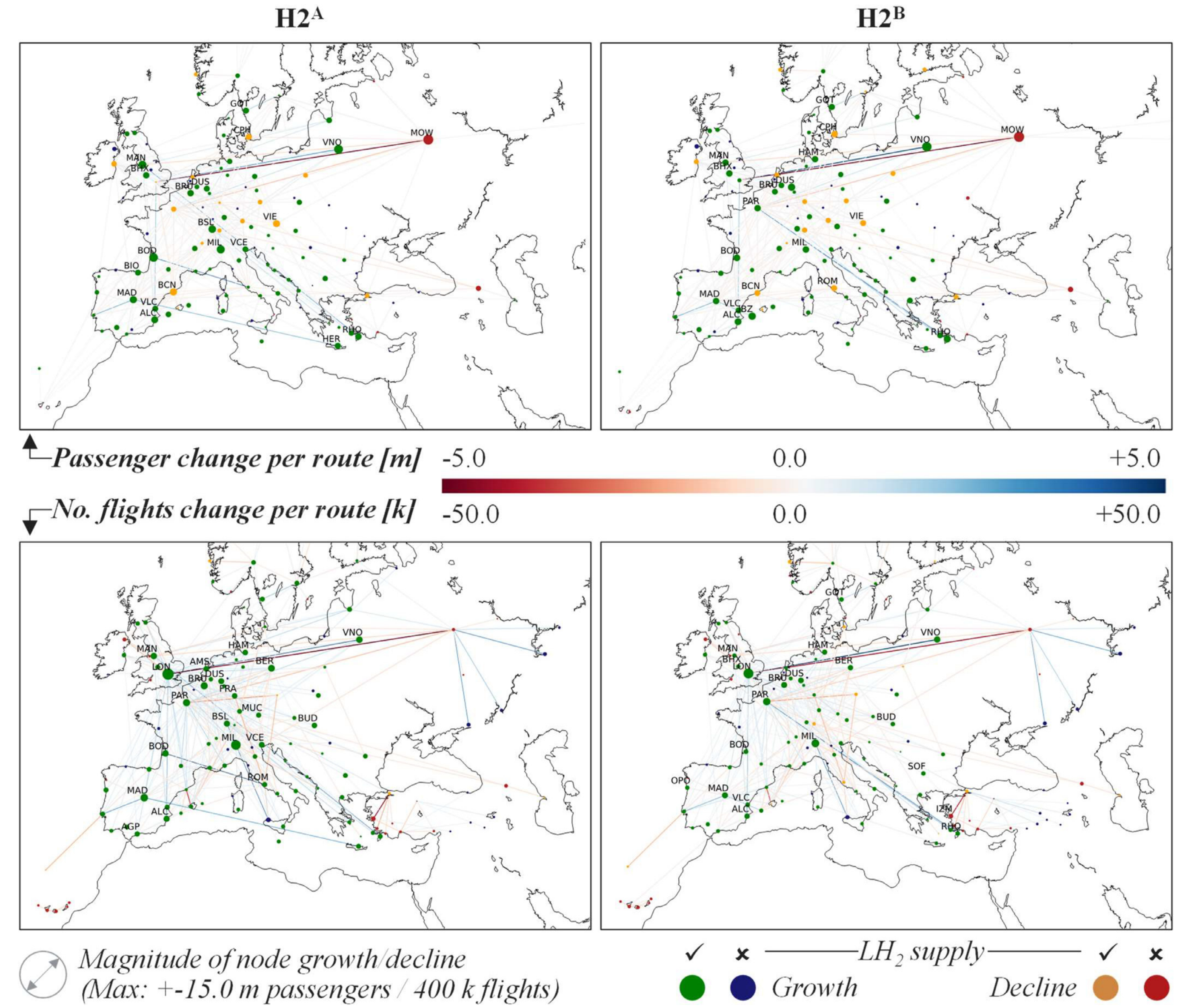

Fig. 16. Intra-European network development resulting from introduction of H2A & H2B (top 300 routes, absolute change).

References

Adler, Eytan J., & Martins, Joaquim R. R. A (2023). Hydrogen-powered aircraft. Fundamental concepts, key technologies, and environmental impacts. *Progress in Aerospace Sciences, 141*, Article 100922. https://doi.org/10.1016/j.paerosci.2023.100922.

Airbus (2020): Airbus reveals new zero-emission concept aircraft. With assistance of Marie-Alix Delestrade. Toulouse, 9/21/2020. Available online at https://www.airbus.com/en/newsroom/press-releases/2020-09-airbus-reveals-new-zero-emission-concept-aircraft, checked on 10/31/2023.

Airbus (5/27/2021): Airbus provides suppliers with an update on production plans. Toulouse. Available online at https://www.airbus.com/en/newsroom/press-releases/2021-05-airbus-provides-suppliers-with-an-update-on-production-plans, checked on 8/4/2021.

Airbus (7/26/2023): Airbus reports Half-Year (H1) 2023 results. Amsterdam. Steuer, Guillaume. Available online at https://www.airbus.com/en/newsroom/press-releases/2023-07-airbus-reports-half-year-h1-2023-results, checked on 8/4/2023.

Airbus (2024): A320neo | Creating higher customer value. Available online at https://aircraft.airbus.com/en/aircraft/a320-the-most-successful-aircraft-family-ever/a320neo-creating-higher-customer-value, checked on 3/20/2024.

Airbus Deutschland GmbH (2003): Liquid Hydrogen Fuelled Aircraft - System Analysis. Final Technical Report.

ATAG (2021): Waypoint 2050. Balancing growth in connectivity with a comprehensive global air transport response to the climate emergency: a vision of net-zero aviation by mid-century. 2nd ed. Air Transport Action Group.

ATR (3/30/2023): ATR set for growth in 2023. Toulouse. Giuria, Charlotte. Available online at https://www.atr-aircraft.com/presspost/atr-set-for-growth-in-2023/, checked on 8/4/2023.

Aviation Week (6/12/2023): Embraer CEO Francisco Gomes Neto Outlines His Revival Plan. Available online at https://aviationweek.com/shownews/paris-air-show/embraer-ceo-francisco-gomes-neto-outlines-his-revival-plan, checked on 8/4/2023.

Bao, Xiaoge, Ji, Peng, Lin, Wei, Perc, Matjaž, & Kurths, Jürgen (2021). The impact of COVID-19 on the worldwide air transportation network. *Royal Society Open Science, 8*(11), Article 210682. https://doi.org/10.1098/rsos.210682.

Baumeister, Stefan (2019). Replacing short-haul flights with land-based transportation modes to reduce greenhouse gas emissions: The case of Finland. *Journal of Cleaner Production, 225*, 262–269. https://doi.org/10.1016/j.jclepro.2019.03.329.

Bhatti, Wasim, Wu, Wei, Doyle, Finn, Llambrich, Jorge, Webber, Helen, Town, Nigel (2022): Fuel Cells Roadmap Report. FlyZero report. FZO-PPN-COM-0033. Aerospace Technology Institute. Available online at https://www.ati.org.uk/wp-content/uploads/2022/03/FZO-PPN-COM-0033-Fuel-Cells-Roadmap-Report.pdf, checked on 1/24/2024.

Birolini, Sebastian, Antunes, António Pais, Cattaneo, Mattia, Malighetti, Paolo, & Paleari, Stefano (2021). Integrated flight scheduling and fleet assignment with improved supply-demand interactions. *Transportation Research Part B: Methodological, 149*, 162–180. https://doi.org/10.1016/j.trb.2021.05.001.

Boeing (2023): Commercial Airplanes Fact Sheet. Available online at https://investors.boeing.com/investors/fact-sheets/default.aspx, updated on 6/30/2023.

Boeing (2024): About the Boeing 737 MAX. Available online at https://www.boeing.com/commercial/737max, checked on 3/20/2024.

Bonnefoy, Philippe, & Weibel, Roland (2006). *Air Transportation System Architecture Analysis*. Cambridge, Massachusetts: Advanced System Architecture. Massachusetts Institute of Technology 2006. Available online at https://ocw.mit.edu/courses/esd-342-advanced-system-architecture-spring-2006/c82a09442f1585c49d32de21a56dfc59_pres1_airtrans.pdf checked on 11/29/2022.

Brewer, G. Daniel (1991). *Hydrogen aircraft technology*. Routledge.

Brons, Martijn, Dijkstra, Lewis, & Poelman, Hugo (2023). *How fast are rail trips between EU cities and is rail faster than air?* (Working papers/Directorate-General for Regional and Urban Policy, WP 2023, 3).

Button, Kenneth, & Stough, Roger (2000). *Air transport networks. Theory and policy implications*. Cheltenham, UK: Edward Elgar (Transport economics, management and policy series).

Cheung, Tommy K. Y., Wong, Collin W. H., & Zhang, Anming (2020). The evolution of aviation network: Global airport connectivity index 2006–2016. *Transportation Research Part E: Logistics and Transportation Review, 133*, Article 101826. https://doi.org/10.1016/j.tre.2019.101826.

Choi, Younseok, & Lee, Jinkwang (2022). Estimation of liquid hydrogen fuels in aviation. *Aerospace, 9*(10), 564. https://doi.org/10.3390/aerospace9100564.

Cirium (2019): Flight schedules and connections data. Available online at https://www.cirium.com/solutions/schedules-and-routes/schedules-and-connections-data/.

Cirium (2020): Fleet Analyzer, 1/1/2020.

Clean Aviation Joint Undertaking (2021): Strategic Research and Innovation Agenda. Version December 2021. Clean Aviation Joint Undertaking. Available online at https://www.clean-aviation.eu/sites/default/files/2022-01/CAJU-GB-2021-12-16-SRIA_en.pdf.

Clean Sky 2 Joint Undertaking (2022): Towards Climate Neutral Aviation. An independent study on the socioeconomic impact of the European Union's Clean Sky 2 Programme. With assistance of Roland Berger, Oxford Economics, **CleanAviation Joint Undertaking.** Clean Sky 2 Joint Undertaking.

Davis, Steven J., Lewis, Nathan S., Shaner, Matthew, Aggarwal, Sonia, Arent, Doug, Azevedo, Inês L., et al., (2018). Net-zero emissions energy systems. *Science (New York, N.Y.), 360*(6396). https://doi.org/10.1126/science.aas9793.

Degirmenci, Hursit, Uludag, Alper, Ekici, Selcuk, & Karakoc, T. Hikmet (2023). Challenges, prospects and potential future orientation of hydrogen aviation and the airport hydrogen supply network: A state-of-art review. *Progress in Aerospace Sciences, 141*, Article 100923. https://doi.org/10.1016/j.paerosci.2023.100923.

Efthymiou, Marina, & Papatheodorou, Andreas (2019). EU emissions trading scheme in aviation: Policy analysis and suggestions. *Journal of Cleaner Production, 237*, Article 117734. https://doi.org/10.1016/j.jclepro.2019.117734.

EIA. (2020). *Annual energy outlook 2020*. U.S. Energy Information Administration Available online at https://www.eia.gov/outlooks/aeo/data/browser/#/?id=12-AEO2020&sourcekey&0 checked on 7/7/2023.

Ekici, Selcuk, Ayar, Murat, & Hikmet Karakoc, T. (2023). Fuel-saving and emission accounting: An airliner case study for green engine selection. *Energy, 282*, Article 128922. https://doi.org/10.1016/j.energy.2023.128922.

European Central Bank (2023): Policy and Exchange Rates. Available online at https://www.ecb.europa.eu/stats/policy_and_exchange_rates/euro_reference_exchange_rates/html/eurofxref-graph-usd.en.html, checked on 05 July, 2023.

European Commission (2020): Sustainable Aviation Fuel - ReFuelEU Aviation. Available online at https://ec.europa.eu/info/law/better-regulation/have-your-say/initiatives/12303-Sustainable-aviation-fuels-ReFuelEU-Aviation_en.

European Environment Agency (2019): EMEP/EEA air pollutant emissions inventory guidebook. Available online at https://www.eea.europa.eu/ds_resolveuid/e0473b3047bf435b95cf245894a9b197, checked on 6/26/2023.

European Union (3/28/2011): Roadmap to a Single European Transport Area – Towards a competitive and resource efficient transport system. COM(2011) 144 final. Available online at https://eur-lex.europa.eu/LexUriServ/LexUriServ.do?uri=COM:2011:0144:FIN:en:PDF, checked on 1/9/2024.

EUROSTAT: Electricity prices for household consumers - bi-annual data (from 2007 onwards) (nrg_pc_204). Available online at https://ec.europa.eu/eurostat/cache/metadata/en/nrg_pc_204_sims.htm, checked on 7/7/2023.

FAA. (2022). *Aerospace forecast. Fiscal years 2022-2042*. Federal Aviation Administration.

Flightglobal (2022): Average weekly jet fuel price from October 2016 to March 2022 (in U.S. dollars per gallon) (Statista). Available online at https://www.statista.com/statistics/526660/aviation-fuel-cost-comparison-across-regions/, checked on 7/5/2023.

Freeman, Linton C. (1977). A Set of Measures of Centrality Based on Betweenness. *Sociometry, 40*(1), 35. https://doi.org/10.2307/3033543.

Fregnani, Jose A., Mattos, Bento S., & Hernandes, José A (2020). An innovative approach for integrated airline network and aircraft family optimization. *Chinese Journal of Aeronautics, 33*(2), 634–663. https://doi.org/10.1016/j.cja.2019.10.004.

Gelhausen, Marc C., Berster, Peter, & Wilken, Dieter (2018). A new direct demand model of long-term forecasting air passengers and air transport movements at German airports. *Journal of Air Transport Management, 71*, 140–152. https://doi.org/10.1016/j.jairtraman.2018.04.001.

Gelhausen, Marc C., Berster, Peter, & Wilken, Dieter (2019). *Airport capacity constraints and strategies for mitigation. a global perspective*. Academic Press.

Gelhausen, Marc Christopher, Berster, Peter, & Wilken, Dieter (2021). Post-COVID-19 Scenarios of Global Airline Traffic until 2040 That Reflect Airport Capacity Constraints and Mitigation Strategies. *Aerospace, 8*(10), 300. https://doi.org/10.3390/aerospace8100300.

Goedeking, Philipp (2010). *Networks in aviation*. Berlin, Heidelberg: Springer Berlin Heidelberg.

Graver, Brandon, Rutherford, Dan, & Zheng, Sola (2020). CO2 emissions from commercial aviation: 2013, 2018, and 2019. International Council on Clean Transportation (ICCT).

Graver, Brandon, Zheng, Sola, Rutherford, Dan, Mukhopadhaya, Jayant, & Pronk, Erik (2022). Vision 2050. Aligning Aviation With The Paris Agreement. Edited by Gary Gardner. International Council on Clean Transportation (ICCT).

Grimme, Wolfgang, Paul, Annika, Maertens, Sven, & van Wensveen, Jasper (2020). The prospects of hybrid-electric regional air transport - an assessment of travel time benefits of domestic short-haul flights in Germany with 19-seater aircraft. *Transportation Research Procedia, 51*, 199–207. https://doi.org/10.1016/j.trpro.2020.11.022.

Guimerà, R., Mossa, S., Turtschi, A., & Amaral, L. A. N. (2005). The worldwide air transportation network: Anomalous centrality, community structure, and cities' global roles. *Proceedings of the National Academy of Sciences of the United States of America, 102*(22), 7794–7799. https://doi.org/10.1073/pnas.0407994102.

Henke, Rolf, Lammering, Tim, & Anton, Eckhard (2010). Impact of an innovative quiet regional aircraft on the air transportation system. *Journal of Aircraft, 47*(3), 875–886. https://doi.org/10.2514/1.45785.

Hess, Stephane (2016). Modelling air travel choice behaviour. In *Airport competition* (pp. 151–175). Routledge. Available online at. https://www.taylorfrancis.com/chapters/edit/10.4324/9781315566481-13/modelling-air-travel-choice-behaviour-stephane-hess.

Hoelzen, Julian, Silberhorn, Daniel, Schenke, Finn, Stabenow, Erik, Zill, Thomas, Bensmann, Astrid, & Hanke-Rauschenbach, Richard (2023). H2-powered aviation – optimized aircraft and green Lh2 supply in air transport networks. DOI: 10.2139/ssrn.4613255.

Hoelzen, Julian, Silberhorn, Daniel, Zill, Thomas, Bensmann, Boris, & Hanke-Rauschenbach, Richard (2022). Hydrogen-powered aviation and its reliance on green hydrogen infrastructure – Review and research gaps. *International Journal of Hydrogen Energy, 47*(5), 3108–3130. https://doi.org/10.1016/j.ijhydene.2021.10.239.

Hoff, Tim, Becker, Florian, Dadashi, Alireza, Wicke, Kai, & Wende, Gerko (2023). Implementation of Fuel Cells in Aviation from a Maintenance, Repair and Overhaul Perspective. *Aerospace, 10*(1), 23. https://doi.org/10.3390/aerospace10010023.

Hospodka, Jakub (2021). Electricity price for aviation. *Transportation Research Procedia, 59*, 253–259. https://doi.org/10.1016/j.trpro.2021.11.117.

Huete, Jon, Nalianda, Devaiah, & Pilidis, Pericles (2021). Propulsion system integration for a first-generation hydrogen civil airliner? *Aeronaut. j, 125*(1291), 1654–1665. https://doi.org/10.1017/aer.2021.36.

Huete, Jon, Nalianda, Devaiah, Zaghari, Bahareh, & Pilidis, Pericles (2022). A Strategy to Decarbonize Civil Aviation: A phased innovation approach to hydrogen technologies. *IEEE Electrific. Mag, 10*(2), 27–33. https://doi.org/10.1109/MELE.2022.3166245.

Hwang, John, & Martins, Joaquim R. R. A (2016). Allocation-mission-design optimization of next-generation aircraft using a parallel computational framework. *57th AIAA/ASCE/AHS/ASC Structures, Structural Dynamics, and Materials Conference. 57th AIAA/ASCE/AHS/ASC Structures, Structural Dynamics, and Materials Conference*. San Diego, California, USA. Reston, Virginia: American Institute of Aeronautics and Astronautics.

IATA (2020a): Air Passenger Market Analysis. December 2019. IATA.

IATA (2020b): World Air Transport Statistics Plus 2020.

IATA (2022): Revenue of commercial airlines worldwide from 2003 to 2021, with a forecast until 2023 (in billion U.S. dollars). Available online at https://www.statista.com/statistics/278372/revenue-of-commercial-airlines-worldwide/, checked on 7/5/2023.

ICAO (2019): Aviation Benefits Report. Available online at https://www.icao.int/sustainability/Documents/AVIATION-BENEFITS-2019-web.pdf.

IEA. (2021). *World energy model documentation*. International Energy Agency.

IPCC (2022): Climate Change 2022. Mitigation of Climate Change.

Janić, Milan (2014). Greening commercial air transportation by using liquid hydrogen (LH 2) as a fuel. *International Journal of Hydrogen Energy, 39*(29), 16426–16441. https://doi.org/10.1016/j.ijhydene.2014.08.011.

Janovec, Michal, Babčan, Viktor, Kandera, Branislav, Šajbanová, Kristína, Škultéty, Filip, & Halvoň, Ľuboš (2023). Performance and weight parameters calculation for hydrogen- and battery-powered aircraft concepts. *Aerospace, 10*(5), 482. https://doi.org/10.3390/aerospace10050482.

Kadyk, Thomas, Winnefeld, Christopher, Hanke-Rauschenbach, Richard, & Krewer, Ulrike (2018). Analysis and design of fuel cell systems for aviation. *Energies, 11*(2), 375. https://doi.org/10.3390/en11020375.

Kallbekken, Steffen, & Victor, David G. (2022). A cleaner future for flight - aviation needs a radical redesign. *Nature, 609*(7928), 673–675. https://doi.org/10.1038/d41586-022-02963-7.

Kanafani, Adib (1981). Aircraft technology and network structure in short-haul air transportation. *Transportation Research Part A: General, 15*(4), 305–314. https://doi.org/10.1016/0191-2607(81)90012-1.

Lee, D. S., Fahey, D. W., Skowron, A., Allen, M. R., Burkhardt, U., Chen, Q., et al., (2021). The contribution of global aviation to anthropogenic climate forcing for 2000 to 2018. *Atmospheric environment, 244*, Article 117834. https://doi.org/10.1016/j.atmosenv.2020.117834.

Ling-Chin, Janie, Giampieri, Alessandro, Wilks, Megan, Lau, Shiew Wei, Bacon, Ellie, Sheppard, Imogen, et al., (2024). Technology roadmap for hydrogen-fuelled transportation in the UK. *International Journal of Hydrogen Energy, 52*, 705–733. https://doi.org/10.1016/j.ijhydene.2023.04.131.

Maertens, Sven, Grimme, Wolfgang, & Bingemer, Stephan (2020). The development of transfer passenger volumes and shares at airport and world region levels. *Transportation Research Procedia, 51*, 171–178. https://doi.org/10.1016/j.trpro.2020.11.019.

Malighetti, Paolo, Paleari, Stefano, & Redondi, Renato (2008). Connectivity of the European airport network: "Self-help hubbing" and business implications. *Journal of air* *transport management, 14*(2), 53–65. https://doi.org/10.1016/j.jairtraman.2007.10.003.

Marksel, Maršenka, & Brdnik, Anita Prapotnik (2023). Comparative analysis of direct operating costs: Conventional vs. Hydrogen fuel cell 19-seat aircraft. *Sustainability, 15*(14), 11271. https://doi.org/10.3390/su151411271.

Meissner, Robert, Sieb, Patrick, Wollenhaupt, Eric, Haberkorn, Stefan, Wicke, Kai, & Wende, Gerko (2023). Towards climate-neutral aviation: Assessment of maintenance requirements for airborne hydrogen storage and distribution systems. *International Journal of Hydrogen Energy, 48*(75), 29367–29390. https://doi.org/10.1016/j.ijhydene.2023.04.058.

Mota, Miguel Mujica, El Makhloufi, Abdel, Boosten, Geert, van Damme, Dick, & Hunt, Ettiene (2017). Is your belly empty?: The analysis of the transition from full freighters to belly cargo Of KLM. *21st Air Transport Research Society Conference, Antwerp*.

Mukhopadhaya, Jayant; Graver, Brandon (2022): Performance Analysis of Regional Electric Aircraft.

Mukhopadhaya, Jayant; Rutherford, Dan (2022): Performance analysis of evolutionary hydrogen-powered aircraft. ICCT white paper.

Newman, M. J. E. (2005). A measure of betweenness centrality based on random walks. *Social Networks, 27*(1), 39–54. https://doi.org/10.1016/j.socnet.2004.11.009.

Oesingmann, Katrin, Grimme, Wolfgang, & Scheelhaase, Janina (2024). Hydrogen in aviation: A simulation of demand, price dynamics, and CO2 emission reduction potentials. *International Journal of Hydrogen Energy, 64*, 633–642. https://doi.org/10.1016/j.ijhydene.2024.03.241.

Prewitz, Marc, Bardenhagen, Andreas, & Beck, Ramon (2020). Hydrogen as the fuel of the future in aircrafts – Challenges and opportunities. *International Journal of Hydrogen Energy, 45*(46), 25378–25385. https://doi.org/10.1016/j.ijhydene.2020.06.238.

Prussi, Matteo, & Lonza, Laura (2018). Passenger aviation and high speed rail: a comparison of emissions profiles on selected european routes. *Journal of Advanced Transportation, 2018*, 1–10. https://doi.org/10.1155/2018/6205714.

Risse, Kristof, Schäfer, Katharina, Schültke, Florian, & Stumpf, Eike (2016). Central Reference Aircraft data System (CeRAS) for research community. *CEAS Aeronaut J, 7*(1), 121–133. https://doi.org/10.1007/s13272-015-0177-9.

Rompokos, Pavlos, Rolt, Andrew, Nalianda, Devaiah, Isikveren, Askin T., Senné, Capucine, Grönstedt, Tomas, & Abedi, Hamidreza (2020). Synergistic technology combinations for future commercial aircraft using liquid hydrogen. *Volume 3: Ceramics; Coal, Biomass, Hydrogen, and Alternative Fuels. ASME Turbo Expo 2020: Turbomachinery Technical Conference and Exposition*. American Society of Mechanical Engineers Virtual, Online, 21.09.2020 - 25.09.2020.

SABRE (2019): MIDT Database. Available online at https://www.sabre.com/products/suites/pricing-and-revenue-optimization/market-intelligence/.

Sacchi, Romain, Becattini, Viola, Gabrielli, Paolo, Cox, Brian, Dirnaichner, Alois, Bauer, Christian, & Mazzotti, Marco (2023). How to make climate-neutral aviation fly. *Nature communications, 14*(1), 3989. https://doi.org/10.1038/s41467-023-39749-y.

Sallan, Jose M., & Lordan, Oriol (2020). Complex networks theory. In *Air route networks through complex networks theory* (pp. 45–69). Elsevier.

Scholz, D., & Thorbeck, J. (2013). *DOC-Assessment Method. A simplified DOC Model. 3rd Symposium on Collaboration in Aircraft Design. TU Berlin* 2013.

Smith, Jessie R., & Mastorakos, Epaminondas (2024). An energy systems model of large commercial liquid hydrogen aircraft in a low-carbon future. *International Journal of Hydrogen Energy, 52*, 633–654. https://doi.org/10.1016/j.ijhydene.2023.04.039.

Stautner, Wolfgang, Ansell, Phillip J., & Haran, Kiruba S (2022). CHEETA: An All-Electric Aircraft Takes Cryogenics and Superconductivity on Board: Combatting climate change. *IEEE Electrific. Mag, 10*(2), 34–42. https://doi.org/10.1109/MELE.2022.3165948.

Sun, Junzi, Hoekstra, Jacco M., & Ellerbroek, Joost (2020). OpenAP: An open-source aircraft performance model for air transportation studies and simulations. *Aerospace, 7*(8), 104. https://doi.org/10.3390/aerospace7080104.

Sun, Xiaoqian; Wandelt, Sebastian; Stumpf, Eike (2018): Competitiveness of on-demand air taxis regarding door-to-door travel time: A race through Europe. In *Transportation Research Part E: Logistics and Transportation Review* 119, pp. 1–18. DOI: 10.1016/j.tre.2018.09.006.

Svensson, Christian; Oliveira, Amir A.M.; Grönstedt, Tomas (2024): Hydrogen fuel cell aircraft for the Nordic market. In *International Journal of Hydrogen Energy* 61, pp. 650–663. DOI: 10.1016/j.ijhydene.2024.02.382.

Tabernier, Laurent; Fernández, Esther Calvo; Tautz, Andreas; Deransy, Robin; Martin, Peter (2021): Fuel Tankering: Economic benefits and environmental impact for flights up to 1500 NM (Full Tankering) and 2500 NM (Partial Tankering). In *Aerospace* 8 (2), p. 37. DOI: 10.3390/aerospace8020037.

Tay, Gilbert; Gillen, Sarah; Rothfeld, Raoul L.; Hornung, Mirko (2018): Evaluation of the Potential Impacts of Hybrid-Electric Aircraft on the Global Air Transportation Network. In : 31st Congress of the International Council of the Aeronautical Sciences, September 09-14. Belo Horizonte, Brazil.

Taylor, Christine, & Weck, Olivier L. de (2007). Coupled vehicle design and network flow optimization for air transportation systems. *Journal of Aircraft, 44*(5), 1479–1486. https://doi.org/10.2514/1.27320.

TEAL (2023): Aircraft Delivery Forecast, 07/2023.

The World Bank (2023): Inflation, consumer prices (annual %). Available online at https://data.worldbank.org/indicator/FP.CPI.TOTL.ZG?end=2019&start=2010&view=chart, checked on 7/5/2023.

Thonemann, Nils; Pierrat, Eleonore; Dudka, Katarzyna Maria; Saavedra-Rubio, Karen; Tromer Dragsdahl, Anna Lia S.; Laurent, Alexis (2024): Towards sustainable regional aviation: Environmental potential of hybrid-electric aircraft and alternative fuels. In *Sustainable Production and Consumption* 45, pp. 371–385. DOI: 10.1016/j.spc.2024.01.013.

Timmons, David; Terwel, Rob (2022): Economics of aviation fuel decarbonization: A preliminary assessment. In *Journal of Cleaner Production* 369, p. 133097. DOI: 10.1016/j.jclepro.2022.133097.

Tiwari, Saurav; Pekris, Michael J.; Doherty, John J. (2024): A review of liquid hydrogen aircraft and propulsion technologies. In *International Journal of Hydrogen Energy* 57, pp. 1174–1196. DOI: 10.1016/j.ijhydene.2023.12.263.

Troeltsch, Florian M.; Engelmann, Marc; Scholz, Anna E.; Peter, Fabian; Kaiser, Jochen; Hornung, Mirko (2020): Hydrogen Powered Long Haul Aircraft with Minimized Climate Impact. In : AIAA AVIATION 2020 FORUM. AIAA AVIATION 2020 FORUM. VIRTUAL EVENT. Reston, Virginia: American Institute of Aeronautics and Astronautics.

Ueckerdt, Falko, Bauer, Christian, Dirnaichner, Alois, Everall, Jordan, Sacchi, Romain, & Luderer, Gunnar (2021). Potential and risks of hydrogen-based e-fuels in climate change mitigation. *Nat. Clim. Chang., 11*(5), 384–393. https://doi.org/10.1038/s41558-021-01032-7.

United States Congress (2022): Inflation Reduction Act. Available online at https://www.whitehouse.gov/cleanenergy/inflation-reduction-act-guidebook/.

University College London: Aviation Integrated Modelling (AIM). With assistance of Andreas W. Schäfer, Lynnette Dray.

Verstraete, Dries (2009). *The potential of liquid hydrogen for long range aircraft propulsion*. Cranfield University Available online at https://dspace.lib.cranfield.ac.uk/handle/1826/4089.

Verstraete, Dries (2013). Long range transport aircraft using hydrogen fuel. *International Journal of Hydrogen Energy, 38*(34), 14824–14831. https://doi.org/10.1016/j.ijhydene.2013.09.021.

Wiener, Peter; Quincey, Rob; Clarke, Harry; Routaboul, Clémence; Grimme, Wolfgang; Maertens, Sven; Classen, Axel (2023): Market Uptake and Impact of Key Green Aviation Technologies. Final Report. Edited by Niclas Dzikus. European Union. Luxembourg. Available online at https://op.europa.eu/en/publication-detail/-/publication/8253ad77-c21f-11ed-8912-01aa75ed71a1.

Wood, Norman; Hales, Michael O.; Taylor, Simon (2023): Notional Aircraft Platforms for Hydrogen Fuel Cell Propulsion. In: AIAA AVIATION 2023 Forum. San Diego, CA and Online. Reston, Virginia: American Institute of Aeronautics and Astronautics.

Yirgu, Kaleab Woldeyohannes; Kim, Amy M. (2021): Aviation fuel and emissions in air markets with interregional passenger leakage. In *Transportation Research Part D: Transport and Environment* 101, p. 103092. DOI: 10.1016/j.trd.2021.103092.

Zanin, Massimiliano, & Wandelt, Sebastian (2023). An overview of network structures and node importance in the global aviation system from the year 2011 to 2022. *JATRS, 1*(1), 63–80. https://doi.org/10.59521/5E2DDEC9FAD4593B.